Phenotypic characterization of *Brachypodium distachyon BdDRM2*-overexpression mutants demonstrates importance of epigenome actors in determining agronomic traits

Luc Anthony Ouellette

Department of Plant Science

McGill University, Montreal

December 2020

A thesis submitted to McGill University in partial fulfillment of the requirements of the degree of Master of Science

This thesis is lovingly dedicated to my mother, Patricia Ouellette.

ABSTRACT

DNA methylation is an important epigenetic modification involved in eukaryotic genome regulation at local and global scales. It is associated with the transcriptional repression of coding and non-coding DNA, as well as changes in chromosome structure. Many complex plant processes including growth, development, environmental stress response and adaptation are connected to changes in DNA methylation landscapes. The DOMAINS REARRANGED METHYLTRANSFERASES (DRMs) are plant-specific *de novo* DNA methyltransferases that target genomic loci through the RNA-directed DNA methylation pathway, though their importance in plant development has yet to be realized—especially for monocots. Since many economically important crops are monocots with large, complex genomes, we report here an analysis of a DRM homolog, *BdDRM2*, and its importance to agronomically relevant traits in the model monocot, *Brachypodium distachyon*. The goals of this work were threefold: first, to validate previously generated transgenic *B. distachyon BdDRM2*-overexpression lines; second, to characterize any developmental phenotypes resulting from *BdDRM2* overexpression in *B. distachyon*; and third, to characterize the impact of *BdDRM2* overexpression on the *B. distachyon* transcriptome. The results herein show that our transgenic *BdDRM2*-overexpression lines have one to two transgenic events depending on the line, accumulate high levels of *BdDRM2* transcripts and that *in vivo* activity of recombinant BdDRM2 is supported by global DNA methylation levels of two to three times that of wild-type. Furthermore, overexpression of *BdDRM2* resulted in pleiotropic effects with notable impacts on stomatal development, root growth and flowering time. Finally, our preliminary analysis of the effects of *BdDRM2*-overexpression on the *B. distachyon* transcriptome has implicated BdDRM2 in glutathione metabolism and transposition in the model monocot and

has provided a wealth of targets for future investigations. Overall, this study has shed light on the importance of the epigenetic contribution to phenotype and genome regulation in monocots.

RÉSUMÉ

La méthylation de l'ADN est une modification épigénétique importante impliquée dans la régulation des génomes eucaryotiques aux niveaux local et global. Elle est associée à la répression transcriptionnelle de l'ADN codant et non codant, ainsi qu'à des modifications de la structure chromosomique. De nombreux processus végétaux complexes, notamment la croissance, le développement, la réponse aux stress environnementaux et l'adaptation, sont liés aux changements dans les profils de méthylation de l'ADN. Les enzymes DOMAINS REARRANGED METHYLTRANSFERASES (DRMs) sont des ADN méthyltransférases *de novo* spécifiques aux plantes qui ciblent des locus génomiques via de petits ARN, mais leur importance dans le développement des plantes n'a pas encore élucidé, en particulier chez les plantes monocotylédones. Étant donné que de nombreuses cultures économiquement importantes sont des plantes monocotylédones avec de grands génomes complexes, nous rapportons ici une analyse d'un homologue DRM, BdDRM2 chez *Brachypodium distachyon*, plante modèle pour les monocotylédones, et son importance pour les caractères agronomiquement pertinents. Les objectifs de ce travail étaient triples: premièrement, valider les lignées de surexpression transgéniques de *B. distachyon* BdDRM2 précédemment générées; deuxièmement, caractériser les phénotypes développementaux résultant de la surexpression de BdDRM2 chez *B. distachyon*; et troisièmement, caractériser l'impact de la surexpression de BdDRM2 sur le transcriptome de *B. distachyon*. Nos résultats montrent que les lignées transgéniques de surexpression de BdDRM2 possèdent un ou deux événements transgéniques selon la lignée et accumulent des niveaux élevés de transcrits BdDRM2. De plus, l'activité *in vivo* de la BdDRM2 recombinante est soutenue par des niveaux globaux de méthylation de l'ADN de deux à trois fois plus élevés chez les lignées transgéniques que chez les plantes de type sauvage. La surexpression de BdDRM2 a aussi entraîné

des effets pléiotropes aux niveaux du développement stomatique, de la croissance des racines et du temps de floraison. Notre analyse préliminaire des effets de la surexpression de BdDRM2 sur le transcriptome de *B. distachyon* implique BdDRM2 dans le métabolisme et la transposition du glutathion dans le modèle monocotylédone et a fourni une multitude de cibles pour de futures enquêtes. Dans l'ensemble, cette étude mets en lumière l'importance de la contribution épigénétique sur le développement des phénotypes chez les plantes monocotylédones.

Table of Contents

LIST OF TABLES AND FIGURES

LIST OF ABBREVIATIONS

5mC: 5-methylcytosine

6MA: N6-methyladenine

ABA: Abscisic acid

ACD: Asymmetric cell division

ACO: 1-aminocyclopropane-1-carboxylic acid oxidase

AGO: ARGONAUTE

bp: Nucleic acid base pairs

CAM: Crassulacean acid metabolism

CG methylation: 5mC DNA methylation in the CG nucleotide sequence context

CHG methylation: 5mC DNA methylation in the CHG nucleotide sequence context, where H = A, C or T nucleotides

CHH Methylation: 5mC DNA methylation in the CHH nucleotide sequence context

CMT: CHROMOMETHYLASE

DCL3: DICER-LIKE 3

DDM1: DECREASE IN DNA METHYLATION

DEG: Differentially expressed gene

DHN: Dehydrin

DIC: Differential interference contrast

DME: DEMETER

DML: DEMETER-LIKE

DMR: Differentially methylated region

DNA: Deoxyribonucleic acid

DPG: Days post germination

DRM: Domains rearranged methyltransferase

ELISA: Enzyme-linked immunosorbent assay

EPF2: EPIDERMAL PATTERNING FACTOR 2

ERF: Ethylene-responsive transcription factor

FAR1: FAR-RED IMPAIRED RESPONSE1

FDM1: FACTOR OF DNA METHYLATION 1

FDR: False discovery rate

FLC: FLOWERING LOCUS C

FWA: FLOWERING WAGENINGEN

GA: Gibberellin

GC: Guard cell

GMC: Guard mother cell

GO: Gene ontology

H3K4me: Histone H3 lysine residue 4 methylation

H3K9me: Histone H3 lysine residue 9 methylation

H3K27me: Histone H3 lysine residue 27 methylation

HEN1: HUA ENHANCER 1

HSE: Heat stress element

Hsf: heat stress transcription factor

HSP: Heat shock protein

kb: Nucleic acid kilo base pairs

LEA: late embryogenesis abundant

MET1: METHYLTRANSFERASE 1

MITE: Miniature inverted repeat transposable element

MS media: Murashige and Skoog media

MTase: Methyltransferase

NCED: 9-*cis*-epoxycarotenoid dioxygenase

ncRNA: non-coding RNA

NLS: Nuclear localization signal

PCR: Polymerase chain reaction

Pol IV: RNA Polymerase IV

Pol V: RNA Polymerase V

PTM: Post-translational modification

RdDM: RNA-directed DNA methylation

RDM1: RNA-DIRECTED DNA METHYLATION 1

RDR2: RNA-DEPENDENT RNA POLYMERASE 2

RGC: Root growth chamber

RNA: Ribonucleic acid

RNAi: RNA interference

RNA-seq: RNA-sequencing

ROS1: REPRESSOR OF SILENCING 1

RT-qPCR: Reverse transcription quantitative PCR

SAM: *S*-adenosyl-L methionine

SC: Subsidiary cell

SHH1: SAWADEE HOMEODOMAIN HOMOLOG 1

SI: Stomatal index

siRNA: small interfering RNA

SUVH: SU(VAR)3-9 HOMOLOG

SUVR: SU(VAR)3-9-RELATED

T-DNA: Transfer DNA

TE: Transposable element

TGS: Transcriptional gene silencing

TSS: transcriptional start site

UBA: Ubiquitin-associated domain

UBI:BdDRM2: transgenic *Brachypodium distachyon BdDRM2*-overexpression lines

UTR: untranslated region

VRN1: VERNALIZATION 1

*ZmUbi*1p: maize ubiquitin-1 promoter

ACKNOWLEDGEMENTS

I would like to begin by acknowledging the great support that my mother and father have provided me with over the years and especially throughout my academic pursuits. To them, I am forever grateful. Thank you, Mom. Thank you, Dad.

I would also like to thank my brother, Marc, and sister, Elise, for aiding and abetting my scientific curiosity through their impressive academic achievements and insights. In other words, I would like to thank them for leaving me no option but to pursue higher education, and for making me laugh. Thanks, Big Guy. Thanks, Little Guy. To my girlfriend, Gabrielle, I don't have enough characters to properly thank you. Simply, thank you for ***everything***.

I would be remiss without thanking my supervisor, Dr. Jean-Benoit Charron, for his incredible insight and guidance with my project, and for his support through challenging times. Thanks, JB.

Thank you also to my committee member, Dr. Jaswinder Singh for his insightful comments; to Dr. Youssef Chebli for his microscopy expertise; and to my lab mates Boris Mayer, Emily Savaria and Hervé Van der Heyden for their encouragement, support and humour.

Lastly, I want to extend my gratitude to the Department of Plant Science at McGill University and the Natural Sciences and Engineering Research Council of Canada for their personal support.

PREFACE

This thesis is composed of original work in its entirety. It is organized and presented here in the traditional monograph style. The contributions of co-authors to this work are detailed below.

Contributions of co-authors:

Chapters I, II and IV were written by Luc Ouellette and Jean-Benoit Charron. Experiments in Chapter III were designed by Luc Ouellette and Jean-Benoit Charron. Calli transformation and generation of transgenic lines for this work were performed previously by Boris Mayer. Transgenic insertion site and global DNA methylation analyses were performed by Luc Ouellette and Boris Mayer. The *Brachypodium distachyon* Root Growth Chambers for root growth analyses were designed by Luc Ouellette and Boris Mayer. Data analysis was performed by Luc Ouellette. Luc Ouellette and Jean-Benoit Charron wrote the Chapter III manuscript.

CHAPTER I: INTRODUCTION

1.1 Introduction

Many abiotic stress-responsive transcription factors and their downstream genes have been identified in plants (Golldack, Lüking, & Yang, 2011; Guo et al., 2016; Lata & Prasad, 2011). Traditional biotechnological breeding approaches such as the overexpression of one or a few stress-responsive genes may not represent a robust strategy for breeding stress-tolerant crops due to the complexity of stress-responsive pathways (Agarwal, Agarwal, Reddy, & Sopory, 2006; H. Wang, Wang, Shao, & Tang, 2016). Although the overexpression of upstream stress-responsive transcription factors shows some promise in improving plant tolerance to various abiotic stresses, it can negatively impact important agronomic traits under normal field conditions (H. Wang et al., 2016). Recently, the importance of plant structure for stress resilience was reported for *B. distachyon* (Mayer, Bertrand, & Charron, 2020). Therefore, understanding how stress-tolerant plants optimize gene expression and development to cope with stress will better assist breeding efforts. Interestingly, increasing evidence points to the regulation of different stress-responsive genes through epigenetic mechanisms (Chinnusamy & Zhu, 2009; Dowen et al., 2012; Mayer, Ali-Benali, Demone, Bertrand, & Charron, 2015; Pandey, Sharma, Sahu, & Prasad, 2016).

DNA cytosine methylation is one such epigenetic modification implicated in plant responses to various stresses (Dowen et al., 2012; Le et al., 2014; Pandey et al., 2016). The up- and down-regulation of genes during plant responses to various environmental stresses is tightly associate with DNA methylation and demethylation dynamics (Viggiano & de Pinto, 2017). DNA methylation is also involved in various aspects of plant growth and development (Y. Li, Kumar, & Qian, 2018; H. Zhang, Lang, & Zhu, 2018). Interestingly, variability in plant morphology and

development can be driven by the differential methylation of genetically identical alleles (i.e. epialleles) and this variability is thought to provide plants with a heritable, yet reversible mechanism for rapid adaptation under selective environments (Cubas, Vincent, & Coen, 1999; Manning et al., 2006; Miura et al., 2009). Since natural intraspecies epigenomic diversity has been shown to correlate with climate and geographical origins (Kawakatsu et al., 2016), epigenetic variation might represent an important tool for adapting crops to the harsher environments predicted by global climate change models.

The level of genomic DNA methylation in plants depends on the combined rates of *de novo* and maintenance methylation, as well as passive and active demethylation (Furner & Matzke, 2011; Matzke & Mosher, 2014). DOMAINS REARRANGED METHYLTRANSFERASES (DRMs) are the main *de novo* DNA methyltransferases in plants such as *Arabidopsis thaliana* (Cao et al., 2003; Cao & Jacobsen, 2002b, 2002a). The *A. thaliana* DRM, DRM2, functions in the RNA-directed DNA methylation (RdDM) pathway, where it specifically catalyzes the *de novo* methylation of DNA cytosine nucleotides in all sequence contexts (CG, CHG and CHH) (Law & Jacobsen, 2010). How DRMs are involved in plant development and responses to abiotic stresses remains largely to be determined.

Previously developed transgenic lines that overexpress a DRM homolog, *BdDRM2*, in the cereal model *Brachypodium distachyon*, have been developed in our lab. The goal of this research project is to characterize the effects of *BdDRM2* misexpression in *B. distachyon* on normal plant growth and development as a first step to uncovering how grasses might change their development in response to various stresses.

1.2 Research hypotheses

1. The *B. distachyon* DRM homologue, *BdDRM2*, controls *de novo* DNA methylation in the model grass. Therefore, constitutive expression of *BdDRM2* under the control of the maize ubiquitin-1 promoter in transgenic *B. distachyon* lines (henceforth, *UBI:BdDRM2*) will result in increased genomic DNA methylation (hypermethylation).
2. DNA methylation is an important component in controlling gene expression and normal growth and development in plants. Therefore, *UBI:BdDRM2* lines will exhibit:
    a. abnormal gene expression and
    b. abnormal developmental phenotypes.

1.3 Objectives

1. Validate transgenic *UBI:BdDRM2* lines by:
    a. Characterizing the number and location of transgene insertions using Genomic DNA sequencing data.
    b. Validating constitutive BdDRM2 expression in *UBI:BdDRM2* lines by assessing transcript accumulation via RT-qPCR and global DNA methylation via ELISA-based analysis.
2. Characterize transcriptome of *UBI:BdDRM2* lines through RNA-sequencing (RNA-seq) analysis.
3. Characterize developmental phenotypes in *UBI:BdDRM2* lines with a focus on traits that have been shown to be affected by changes in DNA methylation in other plant species.

CHAPTER II: LITERATURE REVIEW

2.1 Chromatin modifications, control of gene expression and epigenetics

2.1.1 What is chromatin?

In eukaryotic cells, genomic DNA is organized in the nucleus into a structure called chromatin, which consists of DNA coiled around "packaging" proteins called histones. More precisely, the structure of chromatin is composed of repeating units of nucleosome core particles, made up of approximately 146 base pairs (bp) of DNA wrapped around a histone octamer containing two each of H2A, H2B, H3 and H4 histone proteins, and each core particle is separated by a string of approximately 10-70 bp of linker DNA (Grigoryev, 2012; Kornberg & Lorch, 1999; Luger, Mäder, Richmond, Sargent, & Richmond, 1997). However, the precise length of linker DNA varies along chromosomes and between different species and cell types (Widom, 1992), and perhaps unsurprisingly, linker DNA length affects the packaging of chromatin into higher-ordered structures (Grigoryev, 2012). An additional histone protein, H1 (the linker histone), binds to the entry/exit sites of the linker DNA on the nucleosome core particle (Hergeth & Schneider, 2015). Interestingly, H1 affects the average distance between nucleosome core particles, i.e. nucleosome repeat length (Woodcock, Skoultchi, & Fan, 2006), and the stability of higher-ordered chromatin structures such as the 30 nm fibre (Robinson & Rhodes, 2006). Structurally, chromatin can take on two different conformations, heterochromatin and euchromatin, and these chromatin states impact transcription and therefore gene expression (Xu, Bai, Duan, Costa, & Dai, 2009). Euchromatin has an open conformation that is amenable to active transcription, where heterochromatin conformation is more closed and less amenable to transcription (Xu et al., 2009). Heterochromatin can be further differentiated into constitutive and facultative heterochromatin.

Constitutive heterochromatin contains a large proportion of repetitive DNA and transposable elements (TEs), and it locates in dense pericentromeric and telomeric chromosomal regions (Schotta, Ebert, Dorn, & Reuter, 2003). On the other hand, facultative heterochromatin is a more dynamic structure that can be thought of as transiently condensed euchromatin (Schotta et al., 2003).

2.1.2 Chromatin and gene expression

Despite its repetitive structure, chromatin landscapes are far from uniform. Each nucleosome contains a mosaic of different chromatin modifications such as DNA cytosine methylation (Law & Jacobsen, 2010) and post-translational modifications (PTMs) of histones (Lawrence, Daujat, & Schneider, 2016), and these can alter both structure and function of chromatin (Bannister & Kouzarides, 2011; Berger, 2007; Jenuwein & Allis, 2001). Some examples of histone PTMs include methylation, acetylation, phosphorylation, ubiquitination and SUMOylation (Berger, 2007). These PTMs can be found on H2A, H2B, H3 and H4 histones, and are often found at specific amino acid residues in their N- and C-terminal tails, such as methylation at lysine 9 of H3 (H3K9me) (Berger, 2007). How particular chromatin modifications affect chromatin structure and function depends on many factors including the specific modification, its context, and other downstream actors that recognize the marks. For example, structurally, DNA cytosine methylation is largely associated pericentromeric heterochromatin, and functionally, it is generally associated with the transcriptional repression of genes and TEs (X. Li et al., 2008; X. Zhang et al., 2006). However, the repressive effects of DNA methylation can be overcome by various mechanisms such as the presence of other activating chromatin marks (X. Li et al., 2008) or through interactions with activating protein complexes (Harris et al., 2018). Similarly,

trimethylation of histone H3 tails at lysine residue 27 (H3K27me3) is associated with gene repression and chromatin compaction (Krause & Turck, 2018), whereas trimethylation of histone H3 tails at lysine residue 4 (H3K4me3) is instead associated with gene activation (X. Liu et al., 2016). How H3K27me3 works to repress genes and alter chromatin structure appears to depend on the action of specific H3K27me3 readers, which are protein complexes that recognize and bind to the modification (Krause & Turck, 2018). Interestingly, the opposing H3K27me3 and H3K4me3 marks have been found to be simultaneously present at silenced or low-expressing genes, and it is thought that the presence of activating H3K4me3 keeps these genes poised for activation (Bernstein et al., 2006; Saleh, Al-Abdallat, Ndamukong, Alvarez-Venegas, & Avramova, 2007). Acetylation of lysine residues on H3 or H4 tails is another PTM that affects chromatin structure and gene expression (Berr, Shafiq, & Shen, 2011). The addition of acetyl groups to positively charged lysine residues neutralizes the charge, thereby reducing the affinity of the associated negatively charged nucleosomal DNA, resulting in a transcriptionally-friendly conformation (Berr et al., 2011). Additionally, histone lysine acetylation readers that affect chromatin structure have also been identified (Marmorstein & Zhou, 2014). To summarize, chromatin landscapes are continuously altered by a host of different tags that affect the fruition of gene expression, and no single mark alone determines gene activity.

2.1.3 Epigenetics

An interesting feature of chromatin modifications is that they can be both reversible and mitotically and meiotically heritable (Berger, 2007; Law & Jacobsen, 2010; Lawrence et al., 2016). The study of the heritability of chromatin modifications is called Epigenetics. An excellent example of a mitotic epigenetic event in certain plants is the process of vernalization, which is the

low temperature-induced competence to flower (Bastow et al., 2004). In winter-annual accessions of *Arabidopsis*, the floral repressor FLOWERING LOCUS C (FLC) is expressed at high levels, which inhibits flowering and maintains vegetative growth (Bastow et al., 2004). Exposure of plants to prolonged periods of cold results in the deposition of repressive H3K27me3 at the *FLC* locus, which downregulates *FLC* transcription for the remainder of the life cycle (Bastow et al., 2004). The H3K27me3-mediated downregulation of *FLC* is mitotically but not meiotically stable, as *FLC* expression is high again in the following generation (Bastow et al., 2004; Michaels & Amasino, 2000). DNA cytosine methylation is also heritable, and its heritability depends on the faithful maintenance of the methylation tags by maintenance DNA methyltransferases in newly synthesized DNA (Law & Jacobsen, 2010). In some cases, the same allele can be inherited with different methylation patterns, which can change its activity without changing the underlying DNA sequence (Henderson & Jacobsen, 2007). Such differentially methylated alleles are called epialleles.

Many naturally occurring epialleles have been identified in plants and this epigenetic variation is thought to contribute to adaptive evolution (Cubas et al., 1999; Durand, Bouché, Perez Strand, Loudet, & Camilleri, 2012; L. He et al., 2018; Manning et al., 2006; Martin et al., 2009; Quadrana et al., 2014; Silveira et al., 2013). One such example is the floral symmetry mutant of *Linaria vulgaris* first characterized by Carl Linnaeus in the 18th century. These *L. vulgaris* mutants show radial floral symmetry, due to heavy methylation of the floral development gene, *Lcyc*, which is not methylated in the bilaterally symmetric wild-type flowers (Cubas et al., 1999). Further evidence for the adaptive value of epialleles comes from examination of DNA methylation patterns in global *Arabidopsis* collections, which were found to be tightly associated with their local geographical conditions (L. He et al., 2018; Kawakatsu et al., 2016). In particular, different

methylation patterns were observed at *NMR19-4*, which mediates leaf senescence by negatively regulating the expression of a downstream gene involved in chlorophyll breakdown during leaf senescence (L. He et al., 2018; Schelbert et al., 2009). Thus, it was hypothesized that altered rates of leaf senescence in specific environments may provide enhanced fitness (Kawakatsu et al., 2016). The production of artificially induced epialleles has also been demonstrated (Akimoto et al., 2007). For example, treatment of rice seeds with 5-azadeoxycytidine to reduce DNA methylation led to the identification of a pathogen resistant line where DNA methylation was erased in the promoter region of a resistance gene normally methylated and silenced in wild type plants (Akimoto et al., 2007). Another epiallele in rice, which confers a dwarf phenotype, spontaneously arose in breeding material at Kyusyu University and has been maintained for close to 100 years (Miura et al., 2009). The stability and beneficial agronomic traits demonstrated by certain epialleles thus makes them an attractive tool for breeding programs, especially since epigenetically silenced genes allow the retention of genetic material (in contrast to gene knockouts), preserving diversity. And recently, a study showed that epigenetically diverse populations of *Arabidopsis* accrue up to 40% more biomass and perform better under competitor and pathogen pressure than epigenetically homogenous populations (Latzel et al., 2013). Therefore, further knowledge of DNA methylation dynamics and epiallele generation may present us with novel breeding strategies that consider retention of genetic diversity.

2.2 DNA methylation

2.2.1 What is DNA methylation?

DNA methylation is a process whereby methyl groups are added onto DNA bases through the action of DNA methyltransferases. This modification can occur on cytosine nucleotides at the

fifth carbon of the pyrimidine ring, or on adenine nucleotides at the sixth nitrogen of the purine ring (C. Zhou et al., 2018). In eukaryotes, 5-methylcytosine (5mC) is the major DNA methylation mark and therefore has been studied more widely than N6-methyladenine (6mA), and because of this, "DNA methylation" is often used synonymously with 5mC in the literature pertaining to eukaryotic systems (Jin, Li, & Robertson, 2011; Law & Jacobsen, 2010; H. Zhang et al., 2018). DNA methylation in prokaryotes is a different story; in bacterial genomes, 6mA is the most common mark, and serves many functions including differentiating genomic DNA from invading foreign DNA (Mohapatra & Biondi, 2017). However, 5mC and an additional methylated cytosine, N4-methylcytosine, can also be found in prokaryotic genomes (Casadesus & Low, 2006). Going forth, this review will focus on 5mC in eukaryotes, especially in plants, therefore, further mention of "DNA methylation" should be interpreted as 5mC.

DNA methylation can be further differentiated by its sequence context. In mammals, 5mC occurs in the genome almost exclusively in the symmetrical CG context (Law & Jacobsen, 2010), however, plant genomes contain 5mC in all possible sequence contexts, i.e., CG, CHG and CHH (where H = A, T, or C nucleotides), though CG is most common (X. J. He, Chen, & Zhu, 2011). The CG and CHG sequence contexts are referred to as "symmetrical DNA methylation", as the methyl group can be attached to the cytosines on both the positive and negative DNA strands, thus providing a simple mechanism (i.e. recognition of hemi-methylated DNA by maintenance DNA methyltransferases) for the methylation to be proliferated in the daughter strands after DNA replication, however, the "asymmetrical" CHH methylation cannot be maintained in this way and therefore must be propagated via the RNA-directed DNA methylation pathway or the DECREASE IN DNA METHYLATION (DDM1) dependent methylation pathway (Le et al., 2014; Zemach et al., 2013).

In plants, the majority of DNA methylation occurs in repetitive DNA sequences and TEs, though genes (promoters and/or gene bodies) can also be methylated (Furner & Matzke, 2011; Mirouze & Vitte, 2014). Pericentromeric heterochromatin, as well as siRNA-producing regions are especially methylated in plants (X. Li et al., 2008; Mirouze & Vitte, 2014; Tan et al., 2016; X. Zhang et al., 2006). In *Arabidopsis thaliana*, genome-wide methylation levels at CG, CHG, and CHH sites of 24%, 6.7%, and 1.7%, respectively, have been observed (Cokus et al., 2008). In plants with larger genomes, these proportions increase, which is connected with increases in genomic TE content (Mirouze & Vitte, 2014). The level of genomic DNA methylation depends on the combined rates of *de novo* DNA methylation (i.e. the initial methylation of unmethylated DNA), maintenance methylation, and passive (i.e. failure of maintenance methylation) or active (i.e. enzymatic base excision) demethylation (Furner & Matzke, 2011; Matzke & Mosher, 2014).

Plant *de novo* DNA methylation is catalyzed by the DOMAINS REARRANGED METHYLTRANSFERASE (DRM) family of DNA methyltransferases (Cao & Jacobsen, 2002b; Wada, Ohya, Yamaguchi, Koizumi, & Sano, 2003). DRM homologues have been identified and characterized in eudicots such as *Nicotiana tabacum* (Wada et al., 2003; X. Zhong et al., 2014) and *Arabidopsis thaliana* (Cao et al., 2003; Cao & Jacobsen, 2002b, 2002a), and monocots such as *Oryza sativa* (Dangwal, Malik, Kapoor, & Kapoor, 2013; Moritoh et al., 2012; Tan et al., 2016) and *Hordeum vulgare* (Radchuk, Sreenivasulu, Radchuk, Wobus, & Weschke, 2005). The *Arabidopsis* genome encodes two DRMs, DRM1 and DRM2, with the latter being the primary *de novo* actor (Cao & Jacobsen, 2002b). Interestingly, DRM1 activity appears to be limited to early seed development (Jullien, Susaki, Yelagandula, Higashiyama, & Berger, 2012). Targeting of DRM2 to specific locations in the genome is accomplished in part by small complementary RNA molecules produced by RNA interference (RNAi) machinery in a process known as the RNA-

directed DNA methylation (RdDM) pathway (Naumann et al., 2011; X. Zhong et al., 2014) (discussed in more detail below). DRM2 is capable of *de novo* methylation in all sequence contexts and contributes to the maintenance of CHG and CHH methylation (Cao et al., 2003; Cao & Jacobsen, 2002b).

Maintenance methylation refers to the stable propagation of methylated DNA into newly synthesized DNA. In plants, the major maintenance DNA methyltransferases are METHYLTRANSFERASE 1 (MET1), a plant homologue of the mammalian DNA (cytosine-5)-methyltransferase 1 (Dnmt1), CHROMOMETHYLASE 2 (CMT2) and CMT3, which catalyze the maintenance of CG, CHH and CHG methylation, respectively (H. Zhang et al., 2018). CMT2 is also capable of maintaining CHG methylation, though not to the extent of CMT3 (Stroud et al., 2014; H. Zhang et al., 2018). Maintenance of CG methylation in mammals by Dnmt1 is assisted by the ubiquitin-like, containing PHD and RING finger domains 1 (UHRF1/NP95) protein, which preferentially binds to hemi-methylated DNA (Bostick et al., 2007). Likewise, targeting of MET1 to hemi-methylated CG sites is hypothesized to occur via interactions with VARIANT IN METHYLATION methylcytosine-binding proteins, which are orthologues of mammalian UHRF1/NP95 (Hye, Pontes, Pikaard, & Richards, 2007; Woo, Dittmer, & Richards, 2008; H. Zhang et al., 2018). Interestingly, the maintenance of CHH and CHG methylation mediated by CMT2 and CMT3 relies on the presence of repressive H3K9me chromatin marks, illustrating well the interplay that can occur between various chromatin marks (Du et al., 2012; Stroud et al., 2014; H. Zhang et al., 2018). This relationship is due to the ability of CMT2 and CMT3 to recognize H3K9me through their bromo adjacent homology and chromo domains, but where CMT3 binds mono-, di-, and tri-methylated H3K9 with equal efficiency, CMT2 shows preference for di- and tri-methylated H3K9 (Du et al., 2012; Stroud et al., 2014).

Active DNA demethylation in plants is performed by DNA glycosylases, which excise 5mC from the DNA strand (H. Zhang et al., 2018). The cleaved DNA strand is then repaired with non-methylated cytosine via the DNA base excision repair pathway (H. Zhang & Zhu, 2012). The *Arabidopsis* genome encodes four DNA demethylases, namely, *DEMETER* (*DME*), *REPRESSOR OF SILENCING 1* (*ROS1*), *DEMETER-LIKE 2* (*DML2*), and *DML3*(Le et al., 2014). DME is favourably expressed in the female gametophytic central cell and male gametophytic vegetative cell and it is involved in regulating the expression of maternally imprinted genes during seed development (Le et al., 2014; H. Zhang et al., 2018). Expression of ROS1, DML2 and DML3 occurs in all vegetative tissues and they are thought to catalyze all other DNA demethylation (Le et al., 2014; H. Zhang et al., 2018). Targeting of DNA demethylases to genomic regions depends on specific chromatin modifications and on recruiting proteins (H. Zhang et al., 2018). For example, DME is targeted to euchromatic AT-rich TEs (Gehring, Bubb, & Henikoff, 2009; Hsieh et al., 2009; Huh, Bauer, Hsieh, & Fischer, 2008; Ibarra et al., 2012), and ROS1 targets TEs near protein coding genes that are enriched in the active acetylated H3K18 (H3K18Ac) and repressive H3K27me3 marks (K. Tang, Lang, Zhang, & Zhu, 2016). Furthermore, other ROS1 targets depend on an anti-silencing protein complex, Increased DNA Methylation (IDM), whose component proteins function in H3K18 acetylation *in planta* (Qian et al., 2014; H. Zhang et al., 2018).

2.2.2 Effects of DNA methylation on gene expression

As briefly discussed above, DNA methylation largely affects gene expression by supressing transcriptional activity (Law & Jacobsen, 2010). Genome-wide DNA methylation analysis in *Arabidopsis* revealed an interesting phenomenon regarding the genic context of DNA methylation. Where DNA methylation within promoters was associated with transcriptional gene

silencing (TGS), DNA methylation within gene bodies was associated with high expression and constitutive activity (X. Zhang et al., 2006). However, these observations might not represent the entire picture. A study in rice looked simultaneously at the DNA methylation, H3K4me2 and H3K4me3 profiles across chromosomes 4 and 10, as well as the centromeres of chromosomes 4 and 8 (X. Li et al., 2008). By comparing various groups of genes with varying amounts of these chromatin marks, they showed that DNA methylation alone was correlated with supressed transcription, but that its suppressive effects could be partially relieved by the presence of H3K4me2 and/or H3K4me3. Furthermore, they showed genes containing DNA methylation only in their promoters had higher transcription than those with DNA methylation in their bodies alone or in both promoter and body, which is at odds with what was reported in *Arabidopsis*. However, since the study in *Arabidopsis* reported only on DNA methylation, it was suggested that the high activity of the genes with body methylation in *Arabidopsis* might be explained by the presence of other activating chromatin marks such as H3K4me3 (X. Li et al., 2008). It is also possible that rice and *Arabidopsis* have different downstream actors (e.g. methyl-binding protein effectors) resulting in different "interpretations" of gene body methylation. An interesting explanation of why gene body, rather than promoter methylation, has a greater suppressive effect on transcription is that DNA methylation might inhibit transcript elongation more so than initiation (X. Li et al., 2008; Lorincz, Dickerson, Schmitt, & Groudine, 2004; Okitsu & Hsieh, 2007). DNA methylation outside of gene bodies can also affect gene expression. In fact, methylated TEs situated near genes often appear to reduce their transcription (Harris et al., 2018; Hollister & Gaut, 2009; Lippman et al., 2004). This phenomenon is likely explained by the spreading of DNA methylation for up to 300 bp (and in some cases, over 3 kb) on either side of TE insertions (Quadrana et al., 2016). Interestingly, a DNA methylation reader complex was recently identified in *Arabidopsis*, which

binds to methylated DNA to overcome such transcriptional repression (Harris et al., 2018). Thus, it appears that plant genomes possess mechanisms to overcome possibly detrimental TE-associated gene silencing.

Though the repressive effects of DNA methylation on transcription seem to be the norm, some interesting exceptions have been studied. For example, upregulation of a floral homeotic gene in *Petunia hybrida* was found to be resultant from RdDM of a particular CG in its second intron (Shibuya, Fukushima, & Takatsuji, 2009). This intron contains a putative negative *cis*-element, and it was suggested that methylation of this element might prevent the binding of a transcriptional repressor. Another example of DNA methylation-induced transcriptional upregulation occurs in the DNA demethylase *ROS1* promoter (Lei et al., 2015). This promoter sequence is targeted by both RdDM and ROS1-mediated active demethylation. In this way, the *ROS1* promoter was suggested to act as a "methylstat" by sensing DNA methylation levels and adjusting *ROS1* expression accordingly (Lei et al., 2015). Changes in DNA methylation in some cases may have little to no effect on gene expression. For example, hypomethylation at *Arabidopsis* peri-/chromo-centric domains in response to pathogen attack was found to alter chromatin structure, but no changes in gene expression were detected (Pavet, Quintero, Cecchini, Rosa, & Alvarez, 2006). It was suggested that DNA methylation-induced structural changes such as these may serve other functions, such as increasing the frequency of genetic recombination at these regions (Pavet et al., 2006). Thus, gene regulation through DNA methylation can be quite dynamic and its precise effects are likely dependent on the genic/genomic context of the methylation.

2.3 DNA Methylation and DRMs

2.3.1 RNA-Directed DNA Methylation Pathway

Two unique plant-specific RNA polymerases (derived from RNA Polymerase II) are crucial for the functioning of the RNA-directed DNA methylation pathway, namely, RNA Polymerase IV (Pol IV) and RNA Polymerase V (Pol V) (Haag & Pikaard, 2011). The RdDM pathway can be conveniently divided into two phases based on the actions of each of these polymerases (Matzke & Mosher, 2014). The first phase of the RdDM pathway involves the generation of small interfering RNAs (siRNAs) through the action of Pol IV. First, Pol IV is recruited to target loci (at least in part) by the SAWADEE HOMEODOMAIN HOMOLOG 1 (SHH1), which recognizes and binds to the repressive H3K9me2 (Law et al., 2013). Interestingly, presence of activating H3K4me3 mark reduces the binding affinity of SHH1 (Law et al., 2013). Once present at some locus, Pol IV begins transcribing single stranded RNA (ssRNA), which is then converted to double stranded RNA through the action of RNA-DEPENDENT RNA POLYMERASE 2 (RDR2) (Matzke & Mosher, 2014). This double stranded RNA is then converted into 24-nucleotide siRNAs by DICER-LIKE 3 (DCL3), and to prevent their degradation, HUA ENHANCER 1 (HEN1) adds methyl groups to their 3' ends (Matzke & Mosher, 2014). Often, siRNAs are generated from the expression of direct or inverted repeats. A single strand of siRNA is then incorporated into one of three ARGONAUTE (AGO) proteins, AGO4, AGO6, or AGO9 (M. Zhou & Law, 2015). Notably, the loading of siRNA into AGO4 occurs in the cytoplasm, and this binding is thought to induce a conformational change, exposing a nuclear localization signal (NLS) within AGO4, which then directs it back to the nucleus (Ye et al., 2012).

Polymerase V recruitment to target loci is possibly aided by the two SU(VAR)3-9 homologs (SUVHs) SUVH2 and SUVH9, which bind to methylated DNA (Z. W. Liu et al., 2014).

Once at its target, Pol V begins transcribing what is assumed to be a scaffold RNA, which is targeted by siRNA-loaded-AGO4/6/9 (Matzke & Mosher, 2014). AGO4/6/9 is linked to DRM2 via RNA-DIRECTED DNA METHYLATION 1 (RDM1), thereby positioning the methyltransferase at the target loci (Matzke & Mosher, 2014). Exactly which strand DRM2 methylates appears to be biased towards the strand of same sense as the siRNA involved (X. Zhong et al., 2014).

2.3.2 DRM2 functional characterization

The plant *de novo* methyltransferases, DRMs, were identified based on their sequence similarity to the mammalian Dnmt3 family of *de novo* DNA methyltransferases (Cao et al., 2000). Eukaryotic methyltransferases have a series of conserved catalytic motifs, numerated I to X, although motifs VII and VIII are not well-conserved in most (Cao et al., 2000). Hence their name, these catalytic motifs are rearranged in the DRM proteins with respect to other class-I eukaryotic methyltransferases, i.e. motifs VI, IX and X are N-terminal to motifs I to V (Cao & Jacobsen, 2002b; Cao et al., 2000).

The crystal structure of the *Nicotiana tabacum* DRM2 homologue, NtDRM, was solved and shown to form a homo-dimer similar to the mammalian Dnmt3a-Dnmt3L heterodimer, and this homo-dimer formation appears to be necessary for full methyltransferase activity(X. Zhong et al., 2014). Despite the rearrangement of its catalytic motifs, the overall structure of NtDRM represents that of the class-I methyltransferase fold, having catalytic and target recognition domains (Schubert, Blumenthal, & Cheng, 2003; X. Zhong et al., 2014). For DNA methylation, as well as other cellular component methylation pathways, *S*-adenosyl-L-methionine (SAM) acts as the methyl-group donor (Mull, Ebbs, & Bender, 2006). Binding of SAM occurs in the NtDRM

catalytic domain and each monomer of the homo-dimer binds its own cofactor (X. Zhong et al., 2014). Unlike the mammalian plant *de novo* methyltransferases, the plant DRMs contain a number of ubiquitin-associated (UBA) domains, which are also found in ubiquitin pathway and DNA repair enzymes (Cao et al., 2000). These domains are not required for methyltransferase activity, as demonstrated by *in vitro* experiments using a truncated NtDRM (X. Zhong et al., 2014). They are, however, necessary for maintenance of DNA methylation at the *MEA-ISR* locus (Henderson et al., 2010), as well as for genome-wide activity in *Arabidopsis* (X. Zhong et al., 2014). Interestingly, DRM2uba mutants show DNA methylation to be more strongly reduced in genomic regions with reduced heterochromatic modifications, suggesting a possible euchromatic targeting function of the UBA domains (X. Zhong et al., 2014). As for cellular localization, NtDRM was shown to localize exclusively in the nucleus (Wada et al., 2003) and its NLS is conserved in other plant DRMs (Cao et al., 2000).

2.4 DNA methylation dynamics in plant development

DNA methylation dynamics are tightly woven with the developmental programming of plants, affecting seed development, vegetative growth, pollen tube formation, stomatal development, flowering, fruit ripening, nodule development, and so on (Y. Li et al., 2018; H. Zhang et al., 2018). This isn't surprising since many DNA methylation mutants show various forms of developmental abnormalities (Cao & Jacobsen, 2002a; Chan et al., 2006; Kankel et al., 2003; Moritoh et al., 2012). And many of the natural and artificial epialleles that have been identified show phenotypes with substantially altered plant morphology (Cubas et al., 1999; Durand et al., 2012; L. He et al., 2018; Manning et al., 2006; Martin et al., 2009; Miura et al., 2009; Quadrana et al., 2014; Silveira et al., 2013). Discussed below are a few examples of how

DNA methylation dynamics participate in plant development with a particular focus on those relating to the RdDM pathway.

Proper endosperm and embryo development seems to rely on gene imprinting, which is the differential expression of parental alleles (Huh et al., 2008; Kinoshita, 1999). Imprinted genes in the endosperm, especially maternally expressed genes, are often characterized by hypomethylation where their allelic counterparts are methylated and silenced (H. Zhang et al., 2018). Seed development and germination see dynamic changes in DNA methylation, especially in the asymmetric context (Kawakatsu, Nery, Castanon, & Ecker, 2017). During dry seed development, massive gains of RdDM-mediated CHH methylation occur, especially within TEs, whereas substantial passive losses of CHH methylation occur during germination, and it is hypothesized that this passive demethylation results from the inability of RdDM to keep up with the rapidity of cell division during germination (Kawakatsu et al., 2017). The RdDM pathway also appears to play important roles in the vegetative development of plants. In *Arabidopsis* meristematic tissues, RdDM components are highly transcribed and this is thought to be important for maintaining TE silencing in new tissues and organs as they develop (Baubec, Finke, Mittelsten Scheid, & Pecinka, 2014). Rice *de novo* DNA methylation mutants show a number of vegetative and reproductive developmental abnormalities such as dwarfism, reduced tillering, delayed heading and sterility (Moritoh et al., 2012). Some of these developmental abnormalities in rice might be explained by the fact that RdDM targets miniature inverted repeat transposable elements (MITEs) adjacent to genes involved in gibberellin and brassinosteroid homeostasis, which are important phytohormones involved in growth and development (Wei et al., 2014). Furthermore, leaf development in rice appears to involve the stable silencing of certain developmental genes after the shoot meristem to leaf transition, and OsDRM2-mediated non-CG methylation appears to

direct the deposition of the repressive H3K27me3 mark to maintain this silencing (S. Zhou et al., 2016). Different aspects of leaf development in maize and *Arabidopsis* also involve DNA methylation dynamics. A survey of maize leaves showed that a number of developmental genes were differentially methylated across the four developmental zones, suggesting a role of DNA methylation in controlling proper leaf development (Candaele et al., 2014). Regulation of leaf stomatal density in *Arabidopsis* is in part controlled by *EPIDERMAL PATTERNING FACTOR 2* (*EPF2*), a negative regulator of stomata formation, whose expression is modulated by DNA methylation levels at a TE within its promoter (Yamamuro et al., 2014). Interestingly, both RdDM and ROS1 target the *EPF2* promoter, suggesting that leaf stomatal density might be optimized via DNA methylation and active demethylation activities (Yamamuro et al., 2014). Recently, a number of transcription factors involved in stomatal development have been identified and characterized in *B. distachyon* (Raissig, Abrash, Bettadapur, Vogel, & Bergmann, 2016). However, how these transcription factors themselves are regulated so precisely to create the tightly woven developmental gradient observed on developing *B. distachyon* leaves (**Figure 2.1**) remains unclear.

DNA methylation has also been implicated in various aspects of reproductive growth and development. *FLOWERING WAGENINGEN* (*FWA*) encodes a transcription factor in *Arabidopsis* that is expressed in germinating seeds but is later silenced in vegetative plants by RdDM of tandem repeats near its transcriptional start site (TSS) (Cao & Jacobsen, 2002b; Soppe et al., 2000). The tandem repeats of epigenetic *fwa* mutants are not methylated and this results in ectopic *FWA* expression, which delays flowering (Soppe et al., 2000). Flower development in rice is likely regulated by DNA methylation, as ectopic expression of a rice homologue of the *Arabidopsis FACTOR OF DNA METHYLATION 1* (*FDM1*), which is involved in RdDM, results in various

floral defects (Tao, Liang, An, & Zhang, 2018). DNA methylation changes also appear to be an important component of vernalization in certain plants (Guzy-Wrobelska et al., 2013; Khan et al., 2013; Sherman & Talbert, 2002). The vernalization process in temperate cereals differs from *Arabidopsis*, as vernalization induces the expression of a floral activator, *VERNALIZATION1* (*VRN1*), rather than the repression of the floral inhibitor *FLC* (Khan et al., 2013). In hexaploid winter wheat, vernalization was shown to induce hypermethylation at non-CG sites in a TE fragment located in the first intron of the *VRN-A1* gene, and this hypermethylation associates with its increased expression (Khan et al., 2013). Precisely how this DNA methylation functions to induce *VRN-A1* expression remains to be determined, however, similarities can be drawn to the regulation of the *Petunia* floral homeotic gene (discussed above), which is also induced by DNA methylation in one of its introns (Shibuya et al., 2009). These observations might suggest a greater role of DNA methylation in the modulation of developmental gene expression in plants through the targeting of specific *cis* regulatory sequences. Genomic integrity of sperm cells in developing pollen is important for proper zygotic development, and this integrity is thought to be maintained through 21-nt siRNAs derived from the vegetative nucleus where TE expression is high and RdDM actors are downregulated (Law & Jacobsen, 2010; Pina, 2005; Slotkin et al., 2009). Lastly, DNA methylation changes have been observed during fruit ripening in plants such as tomato (S. Zhong et al., 2013). Specifically, active DNA demethylation takes place in the promoters of various ripening genes, which harbor binding sites of an important ripening transcription factor (S. Zhong et al., 2013). Interestingly, tomato fruit epigenomes contain higher CHH methylation levels than leaf epigenomes, and TEs remain methylated despite massive ripening-associated active demethylation (S. Zhong et al., 2013). This evidence might suggest that RdDM is important in modulating gene and TE expression in ripening tomato fruit.

All this is to say that plant growth and development requires the precise spatiotemporal control of gene expression while maintaining genome integrity, and DNA methylation dynamics (often in concert with other chromatin modifications) appear to be a common mechanism for such control in plants.

2.5 Molecular responses to heat and drought stresses

Heat and drought stresses are particularly challenging for plants and they are responsible for massive (up to 50%) crop yield losses (Lamaoui, Jemo, Datla, & Bekkaoui, 2018). These losses result because heat and drought stresses affect a number of important plant processes. For example, photosynthetic efficiency is drastically reduced under heat and osmotic stresses, which is in part due to stress-induced stomatal closure, inhibited leaf expansion and malfunctioning of the photosynthetic machinery (Lamaoui et al., 2018). Because of their sessile nature, plants have had to adapt a variety of mechanisms for dealing with such stresses to ensure attenuation of the impact on growth, development, and ultimately reproductive success (Viggiano & de Pinto, 2017). Among the mechanisms plants employ to deal with such stresses are many developmental, physiological and biochemical changes that are induced by stress-responsive genes, and these genes are in turn regulated by various networks of transcription factors (Guo et al., 2016).

The dehydration-responsive element binding (DREB) proteins are transcription factors involved in plant responses to dehydrative stresses such as cold and drought. As their name suggests, DREBs bind to dehydration-responsive elements (DREs), which contain the core sequence A/GCCGAC, and thus induce gene expression in response to such stresses (Yamaguchi-Shinozaki, 1994). DREs are found in the promoters of numerous plant stress-responsive genes such as the late embryogenesis abundant (LEA) proteins, which include the dehydrins (DHNs)

(Lata & Prasad, 2011). Although LEA proteins normally amass in seeds late in development, dehydrative stresses see the accumulation of DHNs in vegetative tissues (Hanin et al., 2011). The precise functions of DHNs are not well understood, however, they are thought to act as chaperones (protecting other proteins from dehydration and misfolding), ion- and radical-binding proteins, as well as "space-fillers" to prevent dehydration-induced cellular collapse (Hanin et al., 2011). The *Arabidopsis* genome encodes two main types of DREBs, DREB1 and DREB2, which are involved in cold and drought signal transduction pathways, respectively, and many homologous genes have been identified in agriculturally important grasses (Lata & Prasad, 2011). In addition to drought, DREB2 transcription factors have also been implicated in responses to heat and salinity stresses in rice and maize (Lata & Prasad, 2011).

The heat stress transcription factors (Hsfs) are involved in responses to heat stress in plants and other organisms, and their downstream targets are the heat shock proteins (HSPs). There are three conserved classes (A, B and C) of Hsfs (Kotak et al., 2007). In plant heat stress responses, HsfA1a and HsfA2 are major actors, with the former being the so called "master regulator", as it triggers the heat stress response via induction of other Hsfs (Qu, Ding, Jiang, & Zhu, 2013). Hsfs bind to the heat stress element (HSE) sequence nGAAnnTTCn, which is found in the promoters of heat-responsive genes. Interestingly, many Hsfs are localized to the cytosol under non-stressful conditions but are imported to the nucleus upon heat exposure (Baniwal et al., 2004; Bharti et al., 2000). There are six families of HSPs, which are differentiated based on their molecular masses in kDa: small HSPs, HSP40, HSP60, HSP70, HSP90 and HSP100 (Guertin & Lis, 2010). The HSP70s are highly conserved proteins that protect cells from heat and other abiotic stresses by acting as chaperones degrading misfolded and truncated proteins (Guo et al., 2015; Wen et al., 2017). In *B. distachyon*, 24 *Hsf* and 29 *HSP70* genes have been thus far identified and they locate

to low density regions of CpG islands (Wen et al., 2017), although what effect this localization has on the expression of these genes remains to be determined.

2.6 DNA methylation dynamics in plant stress responses

DNA methylation in plants appears to be dynamically regulated in response to various stresses. In particular, numerous reports demonstrate altered global and site-specific DNA methylation patterns in response to pathogen attack (Le et al., 2014; Wada, Miyamoto, Kusano, & Sano, 2004), mechanical stress (Galaud, Gaspar, & Boyer, 1993), heavy metal toxicity (Aina et al., 2004), cold stress (Steward, Ito, Yamaguchi, Koizumi, & Sano, 2002), salinity stress (Song et al., 2012), heat stress (Gao et al., 2014; Sanchez & Paszkowski, 2014), drought stress (W. Wang et al., 2016; W. S. Wang et al., 2011), etc. These changes include both increased and decreased methylation. For example, the facultative halophyte *Mesembryanthemum crystallinum* switches from C3-photosynthesis to crassulacean acid metabolism (CAM) to adapt to salt-stress and this switch is associated with increased genomic levels of CHG methylation and hypermethylation of satellite regions (Dyachenko et al., 2006). Furthermore, decreased methylation of stress-responsive genes is often associated with their upregulation, and this demethylation often occurs in gene promoters, especially those containing repeat, TE or TE-like sequences (Le et al., 2014; Sanchez & Paszkowski, 2014; Song et al., 2012; Steward et al., 2002; X. Tang, Wang, & Huang, 2018; Wada et al., 2004). However, the precise effect of DNA methylation changes on stress-responsive gene expression seems to vary depending on the locus, as both positive and negative correlations between DNA methylation and transcript abundance have also been observed (W. Wang et al., 2016). As site-specific detection of DNA methylation is improving, studies are finding that transcription factors are often the targets of DNA methylation/demethylation activities (Song et

al., 2012; W. Wang et al., 2016). For example, soybean under salt stress showed demethylation of salt-responsive transcription factors including two DREB transcription factors, which corresponded with their increased expression (Song et al., 2012). Lastly, stress-induced DNA methylation changes are not always associated directly with changes in gene expression, and it is it thought that hypo/hypermethylation of repetitive regions of chromatin or centromeres might occur largely for inducing specialized chromatin structures (Dyachenko et al., 2006; Pavet et al., 2006).

Comparisons between stress-tolerant and stress-sensitive plants have revealed interesting insights regarding DNA methylation dynamics and stress tolerance. In rapeseed (*Brassica napus* L.) seedlings, heat-tolerant and heat-sensitive lines showed DNA methylation increases in leaves during heat stress, however, the DNA methylation increases were higher in the heat-sensitive line compared to the tolerant line (Gao et al., 2014). Furthermore, the heat-tolerant line showed more demethylation events than the sensitive line. Similar studies in rice showed a drought-tolerant line to have 80% more DNA methylation sites at tillering in root tissue compared to a drought sensitive line (W. S. Wang et al., 2011). Moreover, at the heading stage, the drought-tolerant line showed around three times and 5 times more demethylation and methylation sites, respectively, in leaf tissue. A follow-up study further showed that the drought-sensitive line had a higher proportion of differentially methylated regions (DMRs) than the tolerant line, which might suggest that DNA methylation stability during stress is important for successful stress responses (W. Wang et al., 2016). Two types of DNA methylation "behaviours" were identified during drought stress/recovery in these rice lines: 70% of stress-induced DMRs reverted to their original methylation state after recovery, where 29% remained changed after recovery (W. S. Wang et al., 2011). Interestingly, the drought-tolerant line showed a higher proportion of reverting DMRs after

recovery (W. S. Wang et al., 2011). However, in some cases, stress-induced DNA methylation changes may contribute to stress-tolerance, as observed for a nitrogen deficiency-induced epiallele in rice that conferred enhanced tolerance to nitrogen deficiency in the progeny of stressed individuals (Kou et al., 2011).

What actors are involved in stress-induced DNA methylation dynamics and how these changes contribute to stress tolerance remain largely to be determined. Since, TEs and repetitive elements are often sites of stress-induced methylation changes (Le et al., 2014; Naydenov et al., 2015; Sanchez & Paszkowski, 2014), it seems likely that the RdDM pathway should be involved. Indeed, many of the key RdDM pathway components are responsive to heat stress in *Arabidopsis*, and rice DRM2 orthologues are upregulated under heavy metal stress (Naydenov et al., 2015; Ou et al., 2012). Moreover, siRNA biogenesis mutants show weakened stress-induced DNA methylation (Boyko et al., 2010). DNA demethylases have been observed to target TEs within the promoters of stress-responsive genes (Le et al., 2014), and some evidence suggests that the crucial RdDM components, Pol IV and V, are involved in directing this site-specific demethylation (Naydenov et al., 2015). RdDM may also be involved in modulating stress-induced retrotransposition. The induction of *ONSEN* retrotransposons as well as the production of *ONSEN* extrachromosomal DNA copies is observed in response to heat stress (Ito et al., 2011). A high frequency of *ONSEN* retrotransposition is observed in the progeny of siRNA biogenesis mutants subjected to heat stress, but not in wild-type plants. A fascinating observation is that genes close to *ONSEN* insertions gain heat-responsiveness, thus stress-induced retrotransposition may provide a mechanism for the development of new stress-responsive networks, which in some instances might lead to enhanced stress tolerance (Ito et al., 2011). Lastly, a new function in heat-stress response was recently discovered for the imprinted gene *SUPPRESSOR OF drm1 drm2 cmt3*

(*SDC*) (Sanchez & Paszkowski, 2014). Normally, *SDC* is silenced via RdDM of tandem repeats within its promoter, and this silencing is essential for proper leaf development in *Arabidopsis* (Sanchez & Paszkowski, 2014). However, under heat stress, *SDC* becomes activated and its expression aids in heat stress recovery (Sanchez & Paszkowski, 2014). Subsequent heat stress treatments demonstrated that the re-silencing of *SDC* is affected by stress repetitions and thus a type of "stress-memory" is retained, but how this memory is written is not completely understood (Sanchez & Paszkowski, 2014). Furthermore, whether *SDC* participates in responses to other stresses remains to be determined.

2.7 Brachypodium distachyon as a model for cereal epigenetics and abiotic stress responses

In recent years, *Brachypodium distachyon* has been established as a model grass. It possesses all the necessary features of a model plant, namely, facile cultivation and transformation, small stature, rapid life cycle, and a small diploid genome (n = ~272 Mbp) consisting of 2n = 10 chromosomes (Draper, 2001; J. P. Vogel et al., 2010). The classical model plant, *Arabidopsis thaliana*, is a dicotyledonous plant that has long been used as a model system in plant science, however, its utility in studying monocotyledons is somewhat limited; this is especially true for studying monocot-specific features such as cell wall composition and biosynthesis (Scholthof, Irigoyen, Catalan, & Mandadi, 2018). *B. distachyon* belongs to the Pooideae subfamily, the largest subfamily of the Poaceae (grass) family (J. P. Vogel et al., 2010). This phylogeny renders *B. distachyon* particularly useful for studying related large-genome cereal crops such as wheat (*Triticum aestivum*), rye (*Secale cereale*) and barley (*Hordeum vulgare*), as well as for studying energy crops, forage and turf grasses (J. P. Vogel et al., 2010).

A wide variety of genetic and genomic resources are now available for researchers studying *B. distachyon* (Mur et al., 2011). An improved annotated reference genome assembly (v3.1) for the accession Bd21 can be found on Phytozome (***https://phytozome.jgi.doe.gov/***), as well as a reference genome for accession Bd21-3. Furthermore, reference genomes for *B. distachyon* relatives including *Brachypodium stacei* (2n = 20), *Brachypodium hybridium* (2n = 30; allotetraploid with sub genomes derived from *B. distachyon* and *B. stacei*) and the perennial *Brachypodium sylvaticum* are also available on Phytozome. A highly efficient *Agrobacterium*-mediated transformation protocol has been established (J. Vogel & Hill, 2008) and additionally, many T-DNA lines have been developed and are publicly available (Bragg et al., 2012; Hsia et al., 2017), thus facilitating functional genomics studies. Recently, a comprehensive *B. distachyon* pan-genome was published, which catalogues the extent of the species' genes, and interestingly, the pan-genome contains about twice as many genes as any given individual (Gordon et al., 2017). All this is to say that there is a wealth of resources that is continuing to amass, which renders *B. distachyon* a convenient system to study the complex cereals that we rely on so heavily for global food security.

Brachypodium distachyon may also present a better model for studying the epigenetic regulation of gene expression in important cereal crops. For example, DNA methylation is more extensive in larger genome grasses like wheat, in which more than 20% of total cytosines are methylated, whereas only 5% of cytosines are methylated in *Arabidopsis* (Viggiano & de Pinto, 2017). As TEs are especially targeted by RdDM, these results are not surprising since 85% of the wheat genome is derived from TEs compared to around 15% in *Arabidopsis* (Joly-Lopez & Bureau, 2014; Wicker et al., 2018). While the TE concentration of the *B. distachyon* genome isn't as high as wheat, it is almost double that of *Arabidopsis* at around 28% (J. P. Vogel et al., 2010).

Because epigenetic silencing mechanisms can affect the expression of genes containing or neighbouring TEs (Wei et al., 2014; Yamamuro et al., 2014), *B. distachyon* may present a more robust model for understanding this regulation.

Whereas genetic bottlenecks have been imposed on crop plants through domestication, *B. distachyon* as a wild, undomesticated species may possess a greater variation of stress responses than wheat or barley (Verelst et al., 2013). Furthermore, it seems likely that the trait uniformity demanded by domestication would have also reduced epigenetic variation, since epigenetic variation can have major phenotypic effects (Manning et al., 2006; Miura et al., 2009). And since the commonly studied *B. distachyon* accessions Bd21 and Bd21-3 originate near Mosul, Iraq (J. Vogel & Hill, 2008), which has a hot semi-arid climate, we might expect to find well-adapted and variable responses to heat and drought stresses at both the genetic and epigenetic levels. Indeed, *B. distachyon* has been established to be a rather drought resilient plant, especially compared to domesticated cereals (Verelst et al., 2013). Therefore, utilizing *B. distachyon* as a model to uncover adaptive stress-responses at both genetic and epigenetic levels may better assist knowledge translation to important cereal crops.

2.8 Conclusion

To conclude, the DRMs are conserved *de novo* DNA methyltransferases in plants that are implicated in the modulation of gene expression throughout plant growth, development and responses to various stresses biotic and abiotic stresses. DNA methylation in plants is highly dynamic and may be more so in large, repetitive genomes such as those of cereal crops. Thus, characterization of BdDRM2 and DNA methylation dynamics in the cereal model *B. distachyon*

will hopefully provide new insights into the role of this epigenetic modification in crop growth and adaptation.

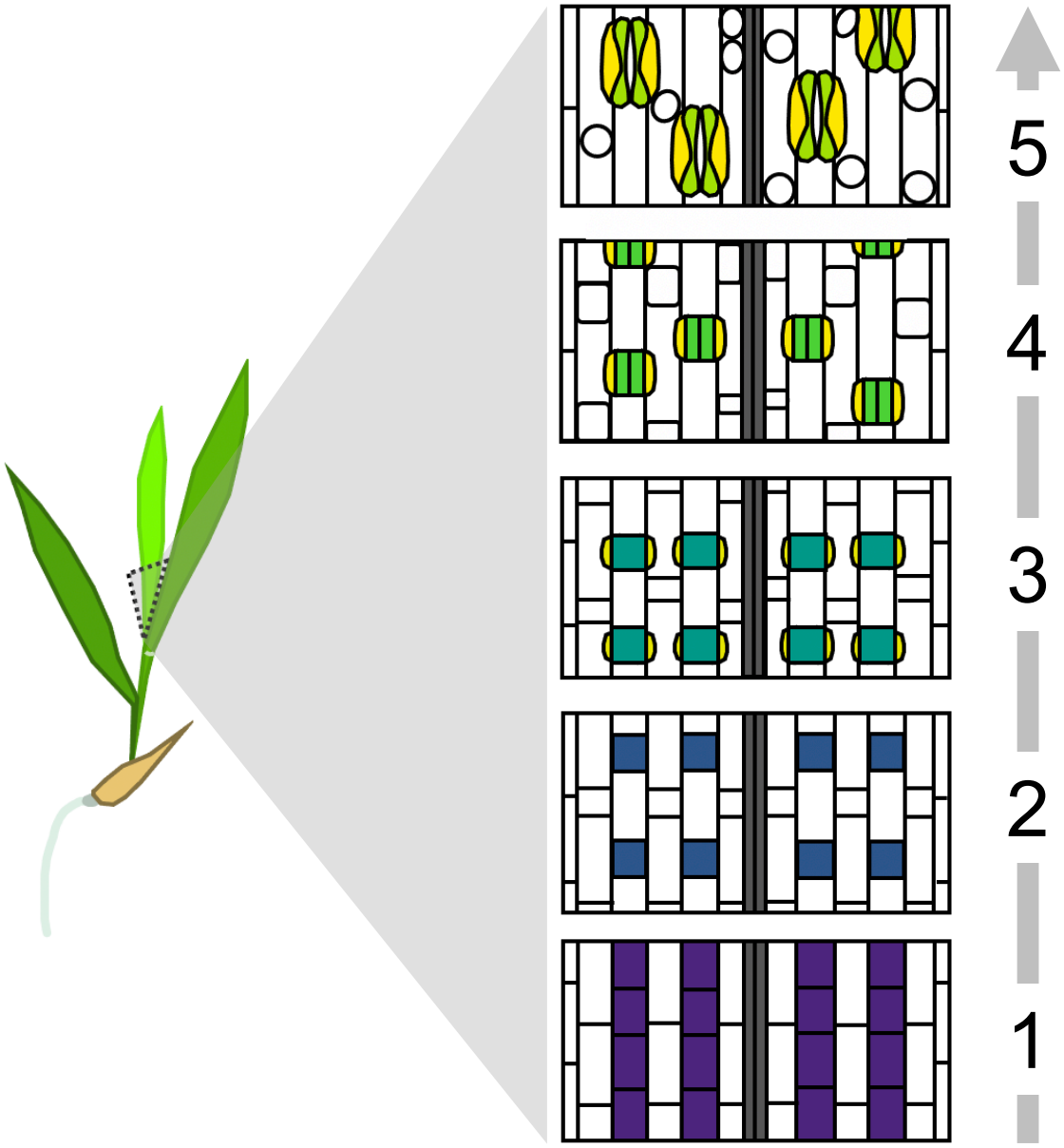

Figure 2.1 Stomatal development in Brachypodium distachyon. Figure modified from Abrash et al. (2018). Mature stomata in *B. distachyon*, like other grasses, are four-celled complexes consisting of two dumbbell-shaped guard cells (GCs) and two flanking lobe-shaped subsidiary cells (SCs). Stomatal development in *B. distachyon* occurs on emerging leaves in a base-to-tip gradient, with cells maturing towards the tip. Development is simplified here in five stages: (**1**) Specific cell files on either side of veins (grey) obtain stomatal lineage fate (purple). (**2**) All epidermal cells undergo asymmetric cell division (ACD). In stomatal files, the smaller cell (blue and teal) of ACD becomes the guard mother cell (GMC); in non-stomatal files, the smaller cell (white) of ACD becomes a hair cell (white circles). (**3**) GMCs recruit SCs (yellow) by inducing ACD in adjacent epidermal pavement cells. (**4**) GMCs divide symmetrically to form two GCs (green). (**5**) GCs and SCs mature as four-celled stomatal complexes, each obtaining their characteristic shapes.

CHAPTER III: RESEARCH FINDINGS

3.1 Materials and methods

3.1.1 Plant material and growth conditions

B. distachyon accession Bd21-3 was used for all experiments as wild-type. The *UBI:BdDRM2* transgenic lines studied in this work were created in the Bd21-3 background.

All seeds were imbibed for 4 hours in distilled water prior to surface sterilization. First, seed lemmas were removed and treated in 70% ethanol with agitation for 1 minute. Following ethanol treatment, seeds were rinsed 3 times in sterile, deionized water and subsequently treated in 1.3% sodium hypochlorite with agitation for 5 minutes. Following sodium hypochlorite treatment, seeds were again rinsed 3 times in sterile, deionized water. Sterilized seeds were then cold stratified in the dark at 4°C in 15 ml falcon tubes double-wrapped with foil for 5-7 days to ensure uniform germination.

Seeds were planted in 2.5 x 2.5-inch pots filled with 80% G2 Agromix (Fafard et Frères Ltd, Saint-Remi, QC, Canada) and 20% sand by volume with a plant density of four seeds per pot. Plants were grown in environmental growth chambers (Conviron, Winnipeg, MB, Canada) at 22°C under 16h photoperiods (16h light/8h dark; 150 μmol m^{-2} s^{-1}) and bottom watered weekly. Pots were randomly distributed in trays, which were rotated in the growth chambers weekly to minimize chamber effects.

For flowering time analyses, plants were first vernalized as planted seeds at 4°C under 8h photoperiods (8h light/16h dark; 150 μmol m^{-2} s^{-1}) for 14 days before being transferred to inductive 16h photoperiods (150 μmol m^{-2} s^{-1}) at 22°C for growth.

For root growth and RNA-seq analyses, plants were grown on full-strength Murashige and Skoog (MS) media containing 1% Phytagel (Sigma-Aldrich) pH 5.8 at 22°C under 16h

photoperiods (150 μmol m^{-2} s^{-1}). Plants were randomly distributed in growth chambers and rotated at least weekly to minimize chamber effects.

3.1.2 Multiple sequence alignment of plant DRMs

To better characterize the *B. distachyon* DRM homologue, BdDRM2, a multiple sequence alignment was performed with previously characterized plant DRMs. Amino acid sequences of *Arabidopsis thaliana* AtDRM2 (Q9M548-1), *Nicotiana tabacum* NtDRM (Q76KU6-1), *Oryza sativa* OsDRM2 (Q10SU5-1) and *Brachypodium distachyon* BdDRM2 (A0A0Q3IJS5-1) were retrieved from the UniProtKB database. The multiple sequence alignment was performed via EMBL-EBI's Clustal Omega tool (Madeira et al., 2019). Data output from Clustal Omega was visualized and annotated using Jalview 2.11.1.3.

3.1.3 Identification of methyltransferase homologues in B. distachyon

To provide further context for our study of BdDRM2, we identified a number of other putative DNA methyltransferases in the *B. distachyon* genome. Amino acid sequences of *de novo* and maintenance DNA methyltransferases characterized in *A. thaliana* were used as queries against the *B. distachyon* genome (taxid:15368) utilizing the Translated BLAST function, tblastn, to identify homologues in *B. distachyon*. The best hit results (lowest E value and highest percent identity) in *B. distachyon* were named according to their *A. thaliana* counterparts. In the case of *B. distachyon* hits not found in *A. thaliana*, genes were named according to the NCBI Reference Sequence Definition. *A. thaliana* DNA methyltransferase queries: AtCMT1 (AT1G80740.1), AtCMT2 (AT4G19020.1), AtCMT3 (AT1G69770.1), AtDRM1 (AT5G15380.1), AtDRM2 (AT5G14620.1), AtDRM3 (AT3G17310.2) and AtMET1 (AT5G49160.1). Identified *B.*

distachyon homologues: *BdCMT1* (BRADI_1g68985v3; XM_010231902.3), *BdCMT2* (BRADI_1g66167v3; XM_014897119.2), *BdCMT3* (BRADI_3g21450v3; XM_010236308.3), *BdDRM2* (BRADI_4g05680v3; XM_010238895.3), *BdDRM3* (BRADI_2g38577v3; XM_003569029.3), BdMET1A (BRADI_1g05380v3; XM_003559258.4) and BdMET1B (BRADI_1g55287v3; XM_024456904.1). For more information, see (**Supplementary Table 3.1**).

3.1.4 DNA methyltransferase tissue expression atlas

To better understand the putative DNA methylation machinery present in *B. distachyon*, a transcript expression atlas was generated. Data for the tissue-specific transcript accumulation of putative *B. distachyon* DNA methyltransferase homologues was obtained from the publicly available Bd21 Expression Atlas (ArrayExpress: experiment E-MTAB-4401) (Davidson et al., 2012) hosted by the European Molecular Biology Laboratory (EMBL-EBI, Hinxton, Cambridgeshire, UK). Expression data in transcripts per million (TPM) was downloaded and visualized with pheatmap in R(R Core Team, 2019).

3.1.5 Generation of transgenic BdDRM2-overexpression lines

Previously, *BdDRM2* cDNA was cloned into the pANIC 6A overexpression vector under the control of the maize ubiquitin-1 promoter (*ZmUbi*1p) (Mann, Lafayette, Abercrombie, Parrott, & Stewart, 2011). The pANIC 6A-*BdDRM2* overexpression vector was transformed into *Agrobacterium tumefaciens* strain AGL1 and subsequently used to transform *B. distachyon* Bd21-3 embryogenic calli using established protocols (J. Vogel & Hill, 2008). T_0 plants were self-fertilized and four distinct, homozygous lines were identified through hygromycin selection. The

resulting *BdDRM2*-overexpression lines (*UBI:BdDRM2*) were named Lines 1 to 4 (L1 to L4) for clarity.

3.1.6 UBI:BdDRM2 transgene insertion site characterization

Genomic DNA was extracted from each of the *UBI:BdDRM2* lines (3 pooled seedlings per line) via phenol: chloroform, and sent for sequencing at Génome Québec. Transgene insertion sites were characterized by following a recently published method for rice (Park et al., 2017). Briefly, Illumina sequencing reads were mapped to the Bd21-3 v1.1 genome obtained from Phytozome (*Brachypodium distachyon* Bd21-3 v1.1 DOE-JGI, ***http://phytozome.jgi.doe.gov***) and to the pANIC 6A overexpression vector (Mann et al., 2011) used to transform the *UBI:BdDRM2* lines in order to characterize *BdDRM2* reads as endogenous, exogenous (transfer DNA sequence plus *BdDRM2*) or plant-transgene integration sites. Results were obtained using Galaxy resources (Galaxy, ***https://usegalaxy.org***) in concert with the Integrative Genomics Viewer (IGV version 2.8.2, Broad Institute and the Regents of the University of California).

3.1.8 Quantitative reverse transcription polymerase chain reaction (RT-qPCR)

To determine transcript accumulation of *BdDRM2* in wild-type and *UBI:BdDRM2* lines, RT-qPCR was performed. Plants at the three-leaf stage were sampled mid-photoperiod. Three biological replicates were collected for analysis. For each biological replicate, aerial tissue was collected from three plants and immediately flash-frozen in liquid nitrogen. RNA was extracted with the EZ-10 RNA kit (cat. no. BS82314; Bio Basic, New York, NY, USA) following the manufacturer's protocol. Extracted RNA was treated with DNase I (cat. no. BS88253; Bio Basic, New York, NY, USA) following the manufacturer's protocol. cDNA was obtained with the iScript

Advanced cDNA Synthesis Kit (cat. no. 1725037; Bio-Rad) following the manufacturer's protocol. RT-qPCR was performed with Green-2-Go (cat. no. QPCR004; Bio Basic, New York, NY, USA) and CFX Connect Real Time (BioRad) following the manufacturers' protocols. Relative transcript levels were determined via ΔΔCT using *UBC18* and *SamDC* as reference genes (Hong, Seo, Yang, Xiang, & Park, 2008).

3.1.9 Global DNA methylation assay

To assess global differences in genomic DNA methylation in wild-type and *UBI:BdDRM2* lines, we performed a global DNA methylation assay. The global DNA methylation assay was performed using the Imprint Methylated-DNA Quantification Kit (Sigma-Aldrich) following the manufacturer's protocol. Genomic DNA was extracted via phenol: chloroform for three independent biological replicates, each consisting of aerial tissue pooled from three plants. Each replicate was measured using a Microplate Reader (Bio-Rad) in technical triplicate.

3.1.10 Abaxial stomata analyses

For all stomata analyses, epidermal imprints of the abaxial surface of the fully expanded third leaf at 18 days post germination was examined. Three biological replicates were analyzed for each line, with each replicate imaged at three non-overlapping regions of the leaf midsection (~2 cm distal and proximal of leaf collar and leaf tip, respectively). Epidermal imprints were created by applying a thin layer of clear nail enamel (Revlon, Clear #771) to abaxial leaf surfaces. Nail enamel was allowed to cure for 1h at room temperature before plant tissue was removed. Cured epidermal imprints were then mounted in water and imaged with a Zeiss Axio Imager Z1

microscope at 20X magnification using a differential interference contrast (DIC) filter. DIC images were analyzed using Fiji ImageJ software (Schindelin et al., 2012).

3.1.11 Root growth analyses

To facilitate long-term observation of *B. distachyon* root growth, sterilized seeds were sown in specialized root growth chambers (RGCs) (**Supplementary Figure 3.1**). The RGCs consisted of three main components: 1) a basal media-containing plant culture box for sterile root growth 2) an apical inverted plant culture box for sterile shoot growth and 3) an opaque basal plant culture box cover to limit root exposure to light. Basal plant culture boxes were filled with ~330 ml (~1 cm below the box lip) of full-strength MS media with 1% Phytagel (wt/vol) and pH adjusted to 5.8. Four sterilized seeds were sown per RGC (one per side). Three layers of porous surgical tape were used to attach and seal the two plant culture boxes. Except when imaging, basal plant culture boxes were covered by black plastic nursery pots and black electrical tape.

RGCs were randomly distributed in environmental growth chambers and rotated every 2-3 days to minimize chamber effects. Root growth was imaged every 2-3 days for 38 days. All images were analyzed using Fiji ImageJ software (Schindelin et al., 2012).

3.1.12 Flowering analyses

Flowering time, expressed as days to heading, was recorded from the time vernalized seeds were transferred to 22°C under 16h photoperiods to the emergence of awns from the flag leaf sheath, i.e. Zadok's 49 (Zadoks, Chang, & Konzak, 1974). Plants were monitored daily at mid-photoperiod for flowering.

3.1.13 RNA-seq analysis

To determine the impact of *BdDRM2* overexpression on the transcriptome, we performed an RNA-seq analysis of *UBI:BdDRM2* Line 3 and wild-type plants. Samples were collected at mid-photoperiod and were immediately flash-frozen in liquid nitrogen. RNA was extracted from two biological replicates, each consisting of three pooled whole seedlings (seed removed) at 8 days post germination (DPG), using the RNeasy Plant Mini Kit (cat. no. 74904; QIAGEN) following the manufacturer's protocol. Libraries were built with NEBNext Multiplex Oligos for Illumina (cat. no. E7600S; New England Biolabs, Ipswich, MA, USA) and sequenced with a NovaSeq 6000 (Illumina) at Centre d'expertise et de services Génome Québec (Montreal, QC, Canada).

RNA-seq analysis was performed using the GenPipes RNA Sequencing Pipeline v3.1.5 (Bourgey et al., 2018) and all jobs were run on the Béluga Compute Canada cluster. Briefly, raw Illumina reads were clipped for adapter sequences, trimmed for minimum quality (Q30) in 3' and filtered for a minimum length of 32 bp using Trimmomatic [PMID: 24695404]. Surviving read pairs were aligned to the **Brachypodium_distachyon_v3.0** genome assembly (available from EnsemblPlants release 49) by the universal RNA-seq aligner STAR [PMID: 23104886] using the recommended two-passes approach. Aligned RNA-Seq reads were assembled into transcripts and their relative abundance was estimated using Cufflinks [PMID: 20436464] and Cuffdiff [PMID: 23222703]. Exploratory analysis was conducted using various functions and packages from R and the Bioconductor project [PMID: 25633503]. Differential expression was conducted using both edgeR [PMID: 19910308] and Deseq [PMID: 20979621]. Terms from the Gene Ontology were tested for enrichment with the GOseq [PMID: 20132535] R package. All of the above processing steps were accomplished through the GenPipes framework [PMID 31185495]. Differentially

expressed genes identified through the pipeline were further filtered for false discovery rate (FDR) adjusted P values < 0.05 and $|\log_2(\text{fold change})| > 1.5$.

At present, *B. distachyon* genome assemblies are currently unavailable through GenPipes resources, thus the Brachypodium_distachyon_v3.0 assembly was installed into our Compute Canada Project space via GenPipes' *install_genome.sh* script. The GenPipes RNA-seq configuration file, *rnaseq.base.ini*, was subsequently modified to call on the Brachypodium_distachyon_v3.0 assembly installed in our project space for the analysis.

3.1.14 Statistical Analyses

Statistical analyses were performed using R (R Core Team, 2019) and JMP 15 software (SAS Institute, Cary, NC, USA). All experimental data were first tested for normality using the Shapiro-Wilk test (shapiro.test R function). Non-normal distributions were tested with a Kruskal-Wallis test (a nonparametric analog of ANOVA; kruskal.test R function) followed by a Dunn's Multiple Comparisons test (dunn.test R function) to assess significance. Normal distributions were tested with a one-way ANOVA followed by the Student's *t*-test in JMP to assess significance of pairwise comparisons. Statistical significance was set at $P < 0.05$.

3.2 Results

3.2.1 B. distachyon BdDRM2 shows sequence homology with other plant DRMs

The amino acid sequence of BdDRM2 (A0A0Q3IJS5-1) was aligned with characterized DRMs from *A. thaliana* (AtDRM2, Q9M548-1), *N. tabacum* (NtDRM, Q76KU6-1) and *O. sativa* (OsDRM2, Q10SU5-1) (**Figure 3.1A**). Sequence similarity was strongest in the regions coding for ubiquitin-associated and SAM-dependent methyltransferase DRM-type domains. Based on

PROSITE-ProRule annotations (AtDRM2 and OsDRM2) and PROSITE-InterPro annotations (NtDRM and BdDRM2), a representation of conserved domain architecture was created for the aligned plant DRMs (**Figure 3.1B**). BdDRM2, like OsDRM2 and NtDRM possesses two UBA domains and a single SAM-dependent methyltransferase DRM-type domain.

3.2.2 The B. distachyon genome encodes homologs of known DNA methyltransferases

Much of the research surrounding DNA methyltransferases in plants has been conducted in *A. thaliana*. To further our understanding of DNA methylation machinery in monocots, the amino acid sequences of characterized *A. thaliana de novo* (*AtDRM1*, *AtDRM2* and *AtDRM3*) and maintenance DNA methyltransferases (*AtMET1*, *AtCMT1*, *AtCMT2*, *AtCMT3*) were used as queries against the *B. distachyon* genome to identify possible *B. distachyon* homologs (**Figure 3.1C**). The *B. distachyon* genome appears to encode two of the three *AtDRM* homologues (*BdDRM2* and *BdDRM3*), an additional *AtMET1* homologue (*BdMET1A* and *BdMET1B*) and all *AtCMT* homologues (*BdCMT1*, *BdCMT2* and *BdCMT3*). Amino acid sequence similarities ranged from 33-55% identity (**Supplementary Table 3.1**).

Utilizing publicly available *B. distachyon* Bd21 transcriptomic resources (Davidson et al., 2012), a tissue-specific expression atlas was generated for the above identified DNA methyltransferase homologs (**Figure 3.1C**). *BdDRM2* transcripts are detected in similar abundances in all examined tissues and share similar expression profiles with *BdCMT2* and *BdDRM3* (**Figure 3.1C**). The putative non-CG methyltransferases, *BdCMT1* and *BdCMT3*, appear to have a degree of tissue-specificity for floral organs as their transcripts are abundantly detected in anthers and pistils, respectively (**Figure3.1C**). Finally, the putative CG-methyltransferase *BdMET1B* is detected in all analyzed tissue libraries, where the paralogous *BdMET1A* is not

detected in leaves or anthers and is otherwise modestly transcribed in the other tissues (**Figure 3.1C**).

3.2.3 Transgenic UBI:BdDRM2 lines have one to two transgene insertions per line

Using genomic DNA sequencing data obtained from the four *UBI:BdDRM2* lines, the number and location of transgene insertions was determined for each transgenic line by mapping sequencing reads to both the *B. distachyon* Bd21-3 genome and the pANIC 6A overexpression vector used to generate the *UBI:BdDRM2* lines (Park et al., 2017). *UBI:BdDRM2* Lines 1 and 3 each have a single transgene insertion, where Lines 2 and 4 each have two transgene insertions (**Figure 3.2A**). More precisely, *UBI:BdDRM2* Line 1 has one insertion at Bd4:37788860; *UBI:BdDRM2* Line 2 has two insertions at Bd3:10392012 and Bd4:16232534; *UBI:BdDRM2* Line 3 has one insertion at Bd3:10231104; and *UBI:BdDRM2* Line 4 has two insertions at Bd2:25458350 and Bd4:37788860 (**Figure 3.2B**). The Bd4:37788860 insertion is present in both Lines 1 and 4, likely indicating that Line 1 was a segregant of early Line 4 generations that lost the Bd2:25458350 insertion (**Figure 3.2A-B**). Although Lines 2 and 3 have insertions on Bd3 in relatively close proximity, they mapped to regions over 150 kilobases apart, lending strong evidence to their uniqueness (**Figure 3.2B**).

Analysis of the genomic context of the five unique *BdDRM2* transgene events revealed Bd3:10392012 (Line 2) and Bd3:10231104 (Line 3) are in regions of the Bd21-3 genome (v1.1) with no annotated features present (**Figure 3.2B**). However, events Bd4:37788860 (Line 1 and 4), Bd4:16232534 (Line 2) and Bd2:25458350 (Line 4) interrupt the 5' UTR of BdiBd21-3.4G0446700.1, an intron of BdiBd21-3.4G0227000.1 and an intron of BdiBd21-3.2G0359000.1, respectively (**Figure3.2B**). According to the Bd21-3 v1.1 genome annotation, BdiBd21-

3.4G0446700.1 encodes a 241 amino acid protein of unknown function DUF1644 (PF07800); BdiBd21-3.4G0227000.1 encodes a 70 amino acid protein with no annotated domains; and BdiBd21-3.2G0359000.1 encodes a 1090 amino acid protein containing six Regulator of chromosome condensation (RCC1) repeats (PF00415), an FYVE zinc finger domain (PF01363), a BREVIS RADIX N-terminal (BRX_N) domain (PF13713), an unstructured region between BRX_N and BRX domains (PF16627) and a BRX domain (PF08381).

3.2.4 Transgenic UBI:BdDRM2 lines accumulate high levels of BdDRM2 transcripts and global DNA methylation

Relative transcript abundance of *BdDRM2* in the *UBI:BdDRM2* lines and wild-type Bd21-3 was analyzed via RT-qPCR and showed that all the transgenic lines displayed significantly higher accumulation of the *BdDRM2* transcript (~18-40 times higher) compared to wild-type (**Figure 3.2C**). Furthermore, ELISA-based analysis of global DNA methylation in the *UBI:BdDRM2* lines revealed an accumulation of two to three times that of wild-type, providing evidence in support of recombinant BdDRM2 activity (**Figure 3.2D**). Interestingly, Line 3 with its single, non-disruptive transgene insertion showed both the highest accumulation of *BdDRM2* transcripts and global DNA methylation (**Figure 3.2A-D**).

3.2.5 Stomatal development is altered by BdDRM2 overexpression

The initiation of stomatal lineage cells has been shown to be affected by DNA methylation changes in *A. thaliana* (Yamamuro et al., 2014). Therefore, in order to determine if this epigenetic modification might also be involved in *B. distachyon* stomatal development, we examined the abaxial surfaces of leaves in the *UBI:BdDRM2* lines for any striking stomatal phenotypes (**Figure**

3.3). Compared to wild-type Bd21-3, all *UBI:BdDRM2* lines showed a significant increase in abaxial stomatal index (SI) (**Figure 3.3A-B**). SI is presented rather than stomatal density as it controls for differences in cell size. During the analysis, it became clear that the development of subsidiary cells (SCs) was affected in the *UBI:BdDRM2* lines, as many SC defects were observed in all transgenic lines (**Figure 3.3C**). The SC defects observed included missing, misshapen, oversized, doublet and triplet SCs (**Figure 3.3C**). No SC defects were observed in wild-type (**Figure 3.3C-D**). Of note again is Line 3, as it showed the greatest density of SC defects (**Figure 3.3D**). Stomatal analyses were conducted on two separate occasions with similar results.

3.2.6 Root growth and architecture are altered by BdDRM2 overexpression

When grown on control (no hygromycin) Murashige and Skoog (MS) plates as part of the selection process, the *UBI:BdDRM2* lines displayed a visible root phenotype compared to wild-type Bd21-3. In order to investigate this further, plants were grown in RGCs on MS media with 1% phytagel (wt/vol) and observed every 2-3 days for ~5 weeks. Compared to wild-type, lateral root growth in the *UBI:BdDRM2* lines appeared severely inhibited and clustered at the primary and seminal root apices by 31 DPG (**Figure 3.4A**). Precise measurement of this phenomenon, however, was complicated by the extent of lateral root clustering in the *UBI:BdDRM2* lines, as well as Bd21-3 root growth beyond the RGC confines at ~24 DPG (**Figure 3.4A**). Measurement of the primary root over 14 days indicated that primary root growth was significantly inhibited in *UBI:BdDRM2* lines compared to wild-type at all points of measurement (**Figure 3.4B**). Root analyses were conducted on two separate occasions with similar results.

3.2.7 Flowering time is delayed by BdDRM2 overexpression

Flowering time of the *UBI:BdDRM2* lines was observed alongside wild-type Bd21-3 under long-day, inductive photoperiods (16h photoperiod at 22°C) after an initial 14-day period of vernalization (8h photoperiod at 4°C) as seed (**Figure 3.5**). All *UBI:BdDRM2* lines exhibited a significant delay in flowering between ~2-4 days on average, however the flowering response was not uniform and showed a prominent right skew (**Figure 3.5A**). The latest flowering wild-type individual took 29 days to reach Zadok's 49 (Zadoks et al., 1974), where some *UBI:BdDRM2* individuals took as long as 38 to 45 days, with others never flowering over the course (56 days) of the experiment (**Figure 3.5A-B**). Flowering time analyses were conducted on three separate occasions with similar results.

3.2.8 The B. distachyon transcriptome is altered by BdDRM2 overexpression

In order to gain further insight into the role of BdDRM2 and *de novo* DNA methylation on *B. distachyon* genome regulation, we performed a preliminary transcriptomic analysis of *UBI:BdDRM2* Line 3 compared to wild-type Bd21-3 under control growth conditions (22°C, 16h photoperiod) at mid-photoperiod. Line 3 was chosen as the representative *UBI:BdDRM2* line due to its single, non-disruptive transgene insertion, its relatively high *BdDRM2* transcript and global DNA methylation accumulation (**Figure 3.2**) and its prominent SC, root and flowering phenotypes (**Figures 3.3-3.5**). Illumina RNA-seq reads were mapped to the Bd21 reference genome (v3.0) and differential expression analysis was conducted via edgeR and Deseq in combination. After further filtering the differential expression results for false discovery rate (FDR) adjusted P values < 0.05 and $|\log_2(\text{fold change})| > 1.5$, a total of 266 differentially expressed genes (DEGs) were identified (**Figure 3.6**). Compared to wild-type, 150 and 116 genes were upregulated and downregulated in

UBI:BdDRM2 Line 3, respectively. Examination of the top 30 DEGs by absolute $\log_2$(fold change) revealed a number of DEGs with either no significant, or uncharacterized BLAST hits found in the *A. thaliana*, *T. aestivum*, *H. vulgare* or *O. sativa* genomes (**Figure 3.6A**). Analysis of the top 30 DEGs by lowest FDR adjusted *P* value confirmed high *BdDRM2* expression in *UBI:BdDRM2* Line 3 compared to wild-type and revealed interesting targets for future investigations (**Figure 3.6B**). Two such targets include BRADI_2g23797v3, a ROS1-like DNA glycosylase (i.e. active DNA demethylase) and BRADI_4g23500v3, a 1-aminocyclopropane-1-carboxylate oxidase (ACO), the rate-limiting enzyme of the ethylene biosynthesis pathway.

DNA methylation has been established as an important factor in contributing to genome stability especially through the silencing of TEs and other repetitive sequences (X. Zhong et al., 2014). Gene ontology (GO) enrichment analysis performed via GO-seq on DEGs (FDR adjusted *P* value < 0.1) showed enrichment in the term *transposition* (GO: 0032196), suggesting that BdDRM2-meadiated DNA methylation may also be important for genome stability in *B. distachyon* (**Figure 3.6C**). Other enriched terms included *glutathione transferase activity* (GO: 0004364) and *glutathione metabolic process* (GO: 0006749), (**Figure 3.6C**). These results might indicate involvement of DNA methylation and/or its machinery in glutathione pathway regulation.

3.2.9 Transcription of other epigenome actors is altered by BdDRM2 overexpression

In addition to BRADI_2g23797v3, the ROS1-like homolog identified above (**Figure 3.6B**), a second ROS1-like homolog, BRADI_4g16620v3, was identified as a DEG in further analysis of the RNA-seq dataset (**Figure 3.7A**). Analysis of amino acid sequence similarity revealed BRADI_2g23797 (henceforth, *BdROS1A*) and BRADI_4g16620 (henceforth, *BdROS1B*) respectively share 56.99% and 56.44% identity with *A. thaliana* ROS1 (AT2G36490)

(**Supplementary Table 3.1**). Interestingly, *BdROS1A* was downregulated in *UBI:BdDRM2* Line 3 where *BdROS1B* was upregulated (**Figure 3.7A-B**). In *A. thaliana*, *ROS1* expression is both positively and negatively regulated by DNA methylation of specific sequences within its promoter (Lei et al., 2015). DNA methylation at a helitron TE within the *ROS1* promoter silences its transcription where DNA methylation at an adjacent short, repetitive "Methylation monitoring sequence" promotes *ROS1* expression. Therefore, to see if similar mechanisms might exist in *B. distachyon* for regulating the expression of DNA demethylation machinery, we searched *BdROS1A* and *BdROS1B* for any annotated repetitive elements (**Supplementary Table 3.2**). No annotated repetitive elements were found within or adjacent to the downregulated *BdROS1A*, however, the upregulated *BdROS1B* contained a number of repetitive elements including a mariner-like TE (trep216) within its presumed promoter region (-394 to -267), another mariner-like TE (trep2027) within its third intron, a *Zea mays*-like unclassified retroelement (Zm_AC148173.2_1L) within its final intron and numerous other short repeats.

The *A. thaliana* histone-lysine N-methyltransferase, Su(var)3-9-related protein 4 (SUVR4), is an important epigenome actor that contributes to genome stability by converting H3K9me1 to H3K9me3 at TEs and pseudogenes, resulting in their transcriptional repression (Veiseth et al., 2011). Interestingly, a SUVR4-like homolog, BRADI_3g48970v3 (henceforth, Bd*SUVR4*), was found in our DEG dataset that showed significant downregulation in *UBI:BdDRM2* Line 3 (**Figure3.7B**).

Finally, a number of non-coding RNAs, which are crucial for the precise targeting of plant DRMs to genomic loci (X. Zhong et al., 2014), were found to be significantly upregulated in *UBI:BdDRM2* Line 3 (**Figure 3.7B**).

3.2.10 BdDRM2 overexpression alters transcription of hormone metabolic genes and plant developmental transcription factors

A number of phytohormone metabolic genes showed altered transcription in *UBI:BdDRM2* Line 3 compared to wild-type. A 1-aminocyclopropane-1-carboxylic acid oxidase-like (ACO-like) homolog, BRADI_4g23500v3, was upregulated in Line 3 (**Figure 3.6B**). Increasing evidence points to ACO as the rate-limiting enzyme of the ethylene biosynthesis pathway (Houben & Van de Poel, 2019). Notably, S-adenosyl methionine is an ethylene precursor that is also used by plant DRMs as the methyl-donor substrate. Other such genes showing altered expression in Line 3 included two significantly downregulated gibberellin (GA) catabolic GA 2-beta-dioxygenase 8-like homologs (BRADI_1g59570v3 and BRADI_5g16040v3), as well as a downregulated homolog of the abscisic acid (ABA) biosynthetic enzyme 9-*cis*-epoxycarotenoid dioxygenase (NCED; BRADI_1g13760v3; **Figure 3.7**). Both GA and ABA are important in many plant development pathways such as seed germination and dormancy in cereals(Tuan, Kumar, Rehal, Toora, & Ayele, 2018), and ABA appears to be the main hormone involved in plant responses to drought (Y. Zhou et al., 2019).

Interestingly, our transcriptomic analysis has uncovered a few potential targets to investigate the developmental phenotypes observed in the *UBI:BdDRM2* lines. Such targets include Line 3-upregulated BRADI_2g21473v3, a FAR-RED IMPARED RESPONSE1 (FAR1)-related sequence, which is a transposase-derived transcription factor important for *A. thaliana* development (Ma & Li, 2018); Line 3-downregulated BRADI_2g49250v3, a zinc finger transcription factor ZAT6-like sequence involved in *A. thaliana* root development and phosphate homeostasis (Devaiah, Nagarajan, & Raghothama, 2007); Line 3 downregulated BRADI_2g166442v3, an ethylene responsive transcription factor (ERF)-like sequence, which are

implicated in both plant development and stress tolerance (Phukan, Jeena, Tripathi, & Shukla, 2017); and the Line 3 upregulated BRADI_3g01250v3 and BRADI_3g01270v3, which are high-affinity nitrate transporter NRT2.1-like sequences shown to be involved in lateral root initiation in *A. thaliana* (Little et al., 2005).

3.2.11 B. distachyon heat shock proteins may be the target of RdDM

Interestingly, our RNA-seq analysis revealed a number of HSPs to be downregulated in Line 3 (**Figure 3.7B**). Analysis of the genomic context of these HSPs revealed a number of repetitive elements within the features (**Supplementary Table 3.2**). These repetitive elements possess many CG, CHG and CHH sites which are often the target of the RdDM pathway. Of the five downregulated HSP-like sequences identified, four contained such repetitive elements, with the exception being BRADI_2g02410v3 (**Supplementary Table 3.2**). However, BRADI_2g02410v3 is directly adjacent to BRADI_2g02400v3, one of the repeat-containing HSP-like sequences, and their similar transcript abundances in Line 3 could suggest their co-regulation.

3.3 Discussion

Much of the current understanding regarding the role of DNA methylation in plant genomes has been elucidated through studies using the model dicot, *A. thaliana* (Law & Jacobsen, 2010). Thus, the role of DNA methylation in grasses is currently limited. To address this issue, we generated transgenic lines overexpressing a DRM homolog, *BdDRM2*, in the model grass *Brachypodium distachyon* (**Figure 3.2**). Previously characterized plant DRMs possess a single DRM-type DNA methyltransferase domain and a variable number of UBA domains (X. Zhong et al., 2014). Alignment of the BdDRM2 amino acid sequence with characterized plant DRMs

indicated a high sequence homology especially in regions coding for UBA and Methyltransferase domains (**Figure 3.1A**). This lends evidence in support of BdDRM2 as a functional *de novo* methyltransferase in *B. distachyon*. To validate our transgenic lines, we assessed the accumulation of *BdDRM2* transcripts and global DNA methylation levels via RT-qPCR and ELISA-based analyses, respectively. Our analyses revealed that the four transgenic *UBI:BdDRM2* lines accumulated significantly higher *BdDRM2* transcripts and global DNA methylation compared to wild-type (**Figure 3.2C-D**).

To give better context for our study, we identified a number of DNA methyltransferase homologs that have been identified in *A. thaliana* (**Supplementary Table 3.1**) and found that *B. distachyon* contains much of the same machinery as *A. thaliana*. Specifically, we found that *B. distachyon* encodes homologs of two of the three *A. thaliana* DRM methyltransferases (DRM2 and the catalytically inactive DRM3), all three CMT methyltransferases, and duplicated copies of the MET1 DNA methyltransferase. Utilizing publicly available tissue-specific transcriptomic data, we showed that *BdDRM2* transcripts are detected in similar abundances throughout *B. distachyon* tissues, and *BdDRM2* shares similar expression profiles with *BdCMT2* and *BdDRM3* (**Figure 3.1C**). We also showed that the putative non-CG methyltransferases, *BdCMT1* and *BdCMT3*, appear to have a degree of tissue-specificity for floral organs as their transcripts are abundantly detected in anthers and pistils, respectively (**Figure3.1C**), perhaps suggesting their involvement in genomic imprinting. Finally, we showed the putative CG-methyltransferase *BdMET1B* is detected in all analyzed tissue libraries, where the paralogous *BdMET1A* is not detected in leaves or anthers and is otherwise modestly transcribed in the other tissues (**Figure 3.1C**). This could suggest diversification of *BdMET1A* function in *B. distachyon*.

As part of a previous project, genomic DNA sequencing data for the four transgenic lines was available and thus used to characterize the number and position of transgene insertions (**Figure 3.2A-B**). Utilizing a recently reported bioinformatics method for mapping transgene insertions (Park et al., 2017), we found that our *UBI:BdDRM2* lines contained one to two insertions per line, for a total of five unique transgenic events. Lines 1 and 3 were found to have single transgene insertions, where Lines 2 and 4 were found to have two insertions. We were also able to assess whether the insertions disrupted any annotated features in the Bd21-3 v1.1 reference genome (**Figure 3.2B**). Two independent transgenic events were found in Lines 2 and 3 that did not disrupt any annotated genomic features. Notably, Line 3 housed a single-copy, non-disruptive transgene insertion and exhibited the highest accumulation of *BdDRM2* transcripts and global DNA methylation. Overall, we have demonstrated that the *UBI:BdDRM2* lines characterized in this study do indeed accumulate high levels of *BdDRM2* transcripts and that recombinant BdDRM2 activity *in planta* is supported by the increased levels of global DNA methylation.

We are particularly interested in the impact of DNA methylation on stress tolerance and agronomic traits in *B. distachyon*, as it is closely related to economically important cereal crops. Recently, the importance of plant architecture in stress tolerance and acclimation was realized in *B. distachyon*, wherein plants exposed to repetitive stresses take on drastically different, stress-minimizing phenotypes (Mayer et al., 2020). Furthermore, repetitive stress treatments in *B. distachyon* transformed the epigenetic landscape of chromatin (Mayer & Charron, 2020). Therefore, as a first step to understanding what role BdDRM2 plays in altering gene expression and growth under stressful conditions, we wanted to characterize any abnormal phenotypes resulting from *BdDRM2* overexpression in control conditions. Indeed, we found alterations to three important agronomic traits: stomatal development, root development and flower timing (**Figures**

3.3-3.5). As stomata and roots directly supply plants with CO_2 and H_2O, the major reactants of photosynthesis, the identification of causal loci for these phenotypes may enhance our knowledge of complex stress-related traits such as carbon fixation and water-use efficiency.

The initiation of stomatal lineage cells has been shown to be affected by the combatting activities of ROS1-mediated DNA demethylation and RdDM in *A. thaliana* (Yamamuro et al., 2014). Although stomatal development in dicots is fundamentally different from monocots, overlap exists between certain *A. thaliana* and *B. distachyon* orthologous transcription factors required for stomatal initiation (Raissig et al., 2016, 2017). Therefore, in order to determine if RdDM might also be involved in *B. distachyon* stomatal development, we examined the abaxial surfaces of leaves in the *UBI:BdDRM2* lines for any striking stomatal phenotypes (**Figure 3.3**). Compared to wild-type, all *UBI:BdDRM2* lines showed a significant increase in abaxial SI (**Figure 3.3A-B**). These results might suggest that DNA methylation also plays a role in determining leaf stomatal populations in *B. distachyon*. Further analysis may uncover actors important for stomatal lineage establishment (see Stage 1 of **Figure 2.1**). In addition to increased SI in the mutants, we observed many peculiar SC defects not present in wild-type (**Figure 3.3C-D**). The missing, misshapen, oversized, doublet and triplet SCs observed in the mutants (**Figure 3.3C**) suggest that SC recruitment and subsequent maturation are defective (see Stage 3 of **Figure 2.1**). More precisely, these defects appear to be resultant from disruptions in ACD. Disruptions to symmetric cell divisions, as in GC formation (see Stage 4 of **Figure 2.1**), were not observed in *UBI:BdDRM2* mutants. Thus, as stomatal development ACDs give rise to GMCs (thus, affecting SI) and SCs (Raissig et al., 2016), our results are consistent with a model where *BdDRM2* overexpression disrupts ACD.

Our transcriptomic analysis of *UBI:BdDRM2* did not reveal any obvious disruptions to known transcription factors involved in *B. distachyon* stomatal development. However, it is likely that our RNA-seq libraries at the scale of whole seedlings are too low-resolution to uncover any potential effects on these actors. Stomatal development in *B. distachyon* occurs in a narrow region at the base of developing leaves, and knowledge of *B. distachyon* stomatal transcription factors comes from fluorescent reporter lines rather than transcript analyses (Raissig et al., 2016). A mobile transcription factor, *BdMUTE*, moves from GMCs to adjacent epidermal pavement cells to induce SC-forming ACDs (Raissig et al., 2017). Thus, to better determine any interactions between BdDRM2 and stomatal transcription factors such as BdMUTE, such reporter lines should be crossed with *BdDRM2* mutants. Future analyses should focus on the developing portion of young leaves to pinpoint the affected stages of stomatal development.

Root development in our *UBI:BdDRM2* lines was drastically altered compared to wild-type (**Figure 3.4**). Specifically, reduced primary root growth (**Figure 3.4B**) and clusters of short lateral roots at seminal and primary root apices (**Figure 3.4A**) were observed. Our transcriptomic analysis of Line 3 compared to wild-type revealed a number of potential targets for future investigations (**Figure 3.7**) These targets include BRADI_2g21473v3, a FAR1-like transposase-derived transcription factor important for *A. thaliana* development (Ma & Li, 2018); BRADI_2g49250v3, a zinc finger ZAT6-like transcription factor involved in *A. thaliana* phosphate homeostasis, primary root growth and development (Devaiah et al., 2007); and BRADI_3g01250v3 and BRADI_3g01270v3, NRT2.1-like high-affinity nitrate transporter sequences shown to be involved in lateral root initiation in *A. thaliana* (Little et al., 2005). Furthermore, ACD is a crucial step in the initiation of lateral roots (Pillitteri, Guo, & Dong, 2016). Thus, the clustering of lateral roots in *UBI:BdDRM2*, taken together with the observed SC defects

discussed above, might suggest a broader role of DNA methylation in ACD in multiple tissues of *B. distachyon*. Indeed, it appears that increasing evidence points to the involvement of epigenetic changes in ACD and cell differentiation (Pillitteri et al., 2016).

The epigenetic regulation of vernalization has been studied in many plant species (Ream, Woods, & Amasino, 2012). Elucidation of the molecular actors and targets of epigenetic remodeling in *B. distachyon* is also well on its way (Huan, Mao, Chong, & Zhang, 2018; Woods et al., 2017). However, whether DNA methylation plays any role in *B. distachyon* vernalization remains unclear. Therefore, we decided to see if flowering time was affected in vernalized *UBI:BdDRM2* mutants (**Figure 3.5**). A modest delay in flowering time was observed in the mutants compared to wild-type (**Figure 3.5A**). These results encourage further analyses including sequence-specific DNA methylation analyses and comparison of the mutants under various vernalization treatments to non-vernalized controls.

Our transcriptomic analysis (**Figure 3.6-3.7**) together with the increased global DNA methylation observed in *UBI:BdDRM2* Line 3 suggests that BdDRM2-mediated DNA methylation is an important component of genomic regulation in *B. distachyon*. The GO enrichment analysis performed on identified DEGs showed enrichment in the terms *transposition* (GO: 0032196), *glutathione transferase activity* (GO: 0004364) and *glutathione metabolic process* (GO: 0006749; **Figure3.6C**). These results suggest that BdDRM2-meadiated DNA methylation may also be important for genome stability in *B. distachyon* through modulation of TEs and other repetitive genetic elements as has been reported for other species (X. Zhong et al., 2014). Further, enrichment of terms glutathione pathway related terms could suggest involvement of epigenetics in the regulation of this pathway, or conversely involvement of glutathione in the epigenome. Interestingly, a connection between glutathione messaging and epigenetic mechanisms has

recently been established in mammals, including S-glutathionylated histone H3 as a new PTM of the histone code (García-Giménez, Romá-Mateo, Pérez-Machado, Peiró-Chova, & Pallardó, 2017).

Our results further suggest the tight connection between different epigenetic actors in *B. distachyon*. Overexpression of *BdDRM2* and the resulting increase in global DNA methylation observed in Line 3 (**Figure 3.2C-D**), taken together with the altered expression profiles of putative *ROS-1*-like DNA glycosylase homologs, *BdROS1A* and *BdROS1B* (**Figure 3.7A-B**), suggests regulation of DNA methylation and demethylation machinery in *B. distachyon* is tightly intertwined as in *A. thaliana*. Repetitive elements identified in the genomic sequence of *BdROS1B* but not *BdROS1A* (**Supplementary Table 3.2**) might indicate a conservation of the *A. thaliana ROS1* DNA methylation-dependent regulatory mechanism for *BdROS1B* expression and a diversification for *ROS1A* regulation. Elucidation of these mechanisms will however require precise analysis of DNA methylation signatures at these loci. Furthermore, disrupted regulation of a histone-lysine N-methyltransferase SUVR4-like homolog in *UBI:BdDRM2* Line 3 might provide insight into *B. distachyon* genome stability (**Figure 3.7B**). In *A. thaliana*, SUVR4 is involved in the silencing of TEs and pseudogenes by converting H3K9me1 in these regions to H3K9me3 (Veiseth et al., 2011). Our results might suggest a similar role for *BdSUVR4* in *B. distachyon* genome stability, and its downregulation in *UBI:BdDRM2* may be compensation for the presumed "over-silencing" effects of *BdDRM2* overexpression. Our transcriptomic analysis also identified a number of upregulated non-coding RNAs (ncRNAs) in *UBI:BdDRM2* Line 3 (**Figure 3.7B**). The precise targeting of plant DRMs to genomic loci is aided by ncRNAs transcribed by Pol V (X. Zhong et al., 2014). Thus, further characterization of these ncRNAs identified could help us to

uncover specific BdDRM2 targets and could possibly explain some of the observed transcriptomic changes.

How overexpression of *BdDRM2* has affected *B. distachyon* growth reported in this study is unclear and requires further work. It will be necessary to identify if any DEGs observed in *UBI:BdDRM2* result from changes to their DNA methylation signatures. This will help pinpoint where BdDRM2's involvement occurs. Possibilities include directly impacting expression of homeotic genes and/or other regulatory genes such as transcription factor networks or phytohormone metabolic genes. Indeed, we found evidence of ethylene, ABA and GA metabolic gene mis-regulation in *UBI:BdDRM2* Line 3 (**Figure 3.7**). Interestingly, DNA methylation and ethylene biosynthesis share SAM as a common substrate. Whether a relationship exists between these pathways or if the upregulation of the rate-limiting ethylene biosynthetic enzyme, ACO, in Line 3 is an artifact of SAM depletion via *BdDRM2* overexpression will be an interesting point to consider for future analyses.

Our transcriptomic analysis also uncovered a number of downregulated HSPs in *UBI:BdDRM2* Line 3 (**Figure 3.7B**). Genome-wide DNA demethylation appears to play an important role in plants during heat stress (Ito et al., 2011; Sanchez & Paszkowski, 2014). Thus, regulation of HSPs by DNA methylation seems likely. Since RdDM targets TEs and repetitive elements, we analyzed the genomic context of the downregulated HSPs identified (**Supplementary Table 3.2**) We found that these HSPs contained a number of repetitive elements that could potentially be targeted by RdDM. Site-specific DNA methylation analysis of these HSPs in *UBI:BdDRM2* lines or in wild-type *B. distachyon* under heat stress will help us determine if indeed a subset of HSPs in *B. distachyon* are regulated by RdDM. Furthermore, heat shock proteins (HSPs) have been recently identified as important components for plant development in wheat

(Kumar et al., 2020). Therefore, the identified HSPs may also help us to uncover the phenotypic abnormalities observed in the *UBI:BdDRM2* lines.

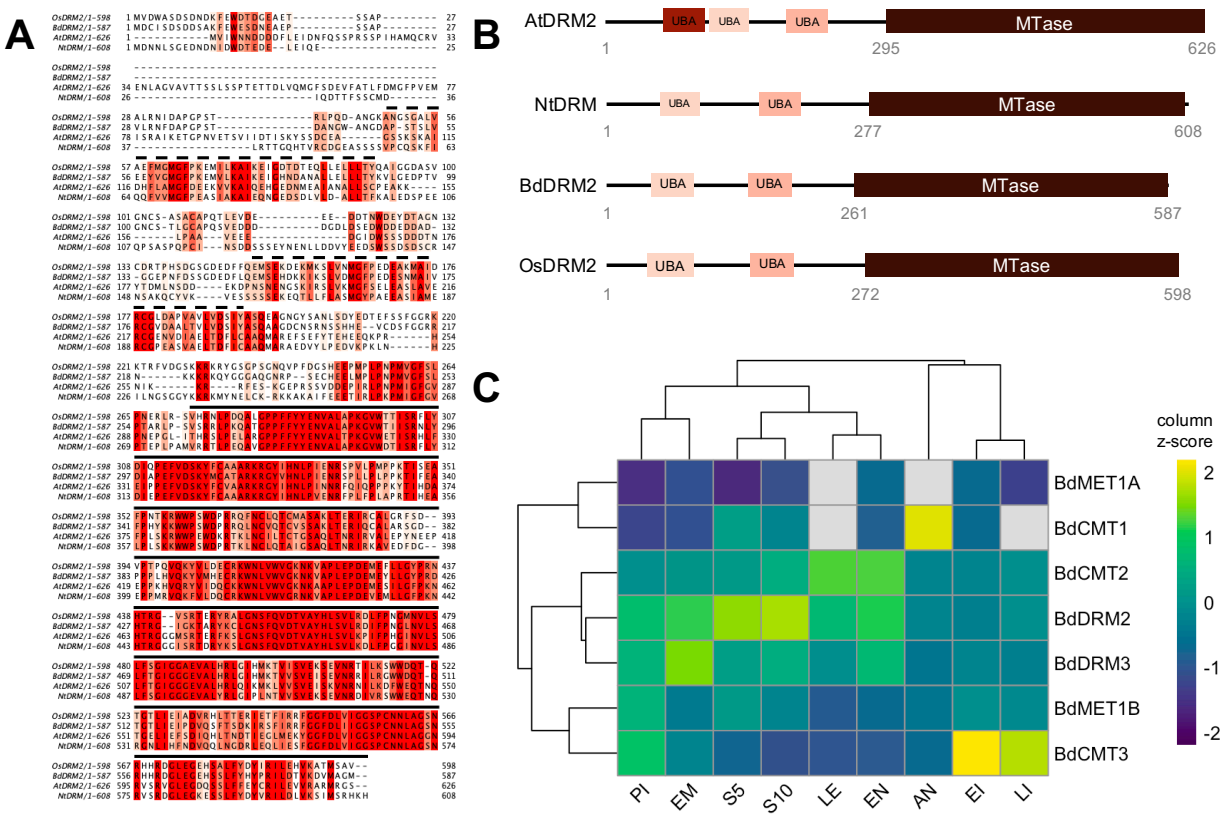

Figure 3.1 BdDRM2 shares homology with other plant DRMs and its transcription is detected in multiple tissues. (A) Multiple sequence alignment of plant DRM amino acid sequences from *Oryza sativa* (OsDRM2), *Brachypodium distachyon* (BdDRM2), *Arabidopsis thaliana* (AtDRM2) and *Nicotiana tabacum* (NtDRM). Conserved amino acid residues (Clustal Omega conservation score > 4.961) are shaded in red with dark red being most conserved (identical) and lighter reds being less conserved. Conserved protein domains are indicated by black bars above alignment (dashed: ubiquitin-associated domain, solid: methyltransferase domain) **(B)** Colour-coded conserved domain architecture of plant DRMs analyzed in (A). DRM methyltransferase domain (MTase) coloured brown, ubiquitin-associated domain (UBA) coloured in shades of red. Like-shaded UBA domains align together as in (A). Numbers below indicate amino acid residue position. **(C)** Transcript profile of DNA methyltransferase-like homologues in various tissues of *B. distachyon* (Bd21) via Bd21 Expression Atlas (Davidson et al., 2012). Transcription of *A. thaliana*-like DNA methyltransferases in pistil (PI), embryo (EM), seed 5 days after pollination (S5), seed 10 days after pollination (S10), leaf (LE), endosperm (EN), anther (AN), early inflorescence (EI) and late inflorescence (LI) is visualized according to column z-core of transcripts per million (TPM) data from *BdMET1A* (BRADI_1g05380v3), *BdCMT1* (BRADI_1g68985v3), *BdCMT2* (BRADI_1g66167v3), *BdDRM2* (BRADI_4g05680v3), *BdDRM3* (BRADI_2g38577v3), *BdMET1B* (BRADI_1g55287v3) and *BdCMT3* (BRADI_3g21450v3) loci; grey colour indicates transcript undetected.

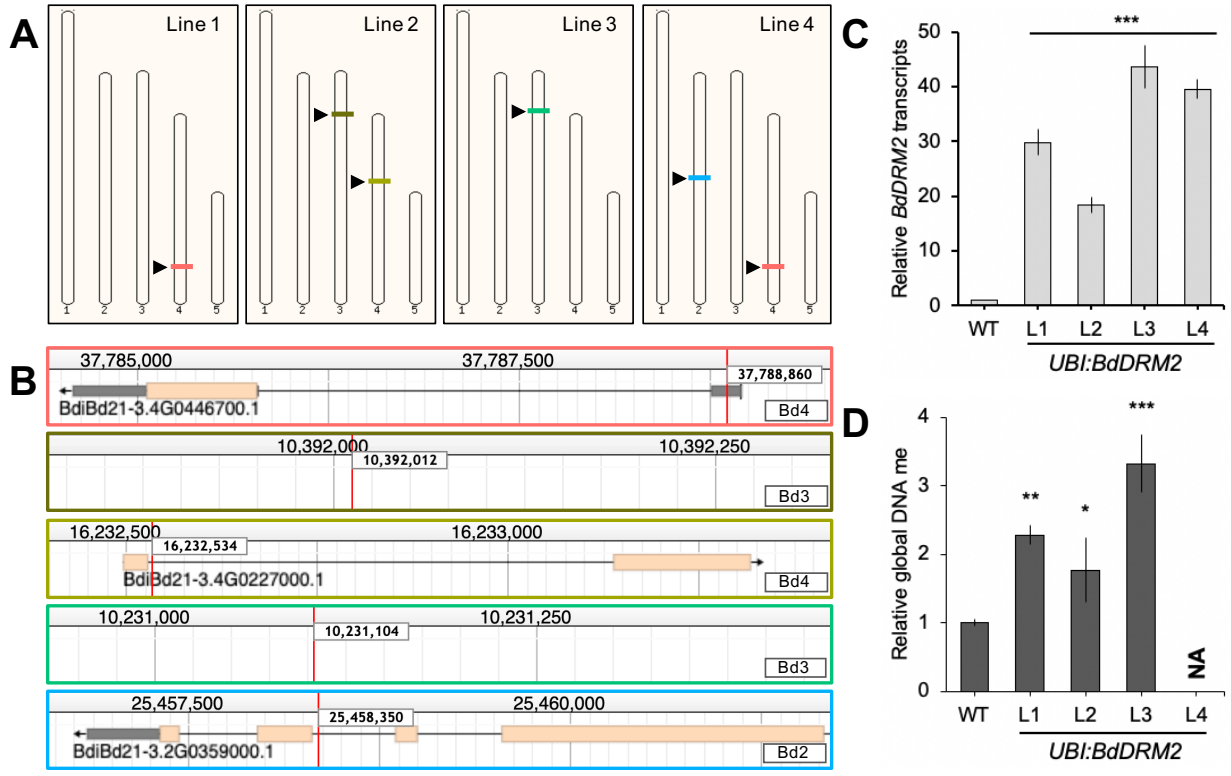

Figure 3.2 Transgenic UBI:BdDRM2 lines show higher *BdDRM2* transcripts and global DNA methylation. (A) Karyotypes of the four transgenic *UBI:BdDRM2* lines showing number and chromosomal location of transgene insertions in the *B. distachyon* Bd21-3 background. Non-unique transgenic events are coloured the same. **(B)** Representation of transgene insertion sites (red lines) in Bd21-3 background showing any annotated transcripts in region. Chromosome number (Bd#) is indicated at lower right. Colours correspond to transgenic events as in (A): red, Bd4:37788860; dark olive, Bd3:10392012; olive, Bd4:16232534; green, Bd3:10231104; blue, Bd2:25458350. **(C)** Relative transcript abundance of *BdDRM2* in wild-type (Bd21-3) compared to *UBI:BdDRM2* lines at 22°C under a 16h photoperiod. Aerial tissue of seedlings at three-leaf stage was collected mid-photoperiod. Bars represent the average of three biological replicates ± 1 SD. ***P<0.0001 **(D)** Relative global DNA methylation in wild-type (Bd21-3) compared to *UBI:BdDRM2* lines at 22°C under a 16h photoperiod. Genomic DNA was extracted from aerial tissue of plants at three-leaf stage. At time of experiment, limited Line 4 plant material prevented its analysis. Bars represent the average of three biological replicates ± 1 SD. *P<0.02; **P<0.001; ***P<0.0001. NA, data not available.

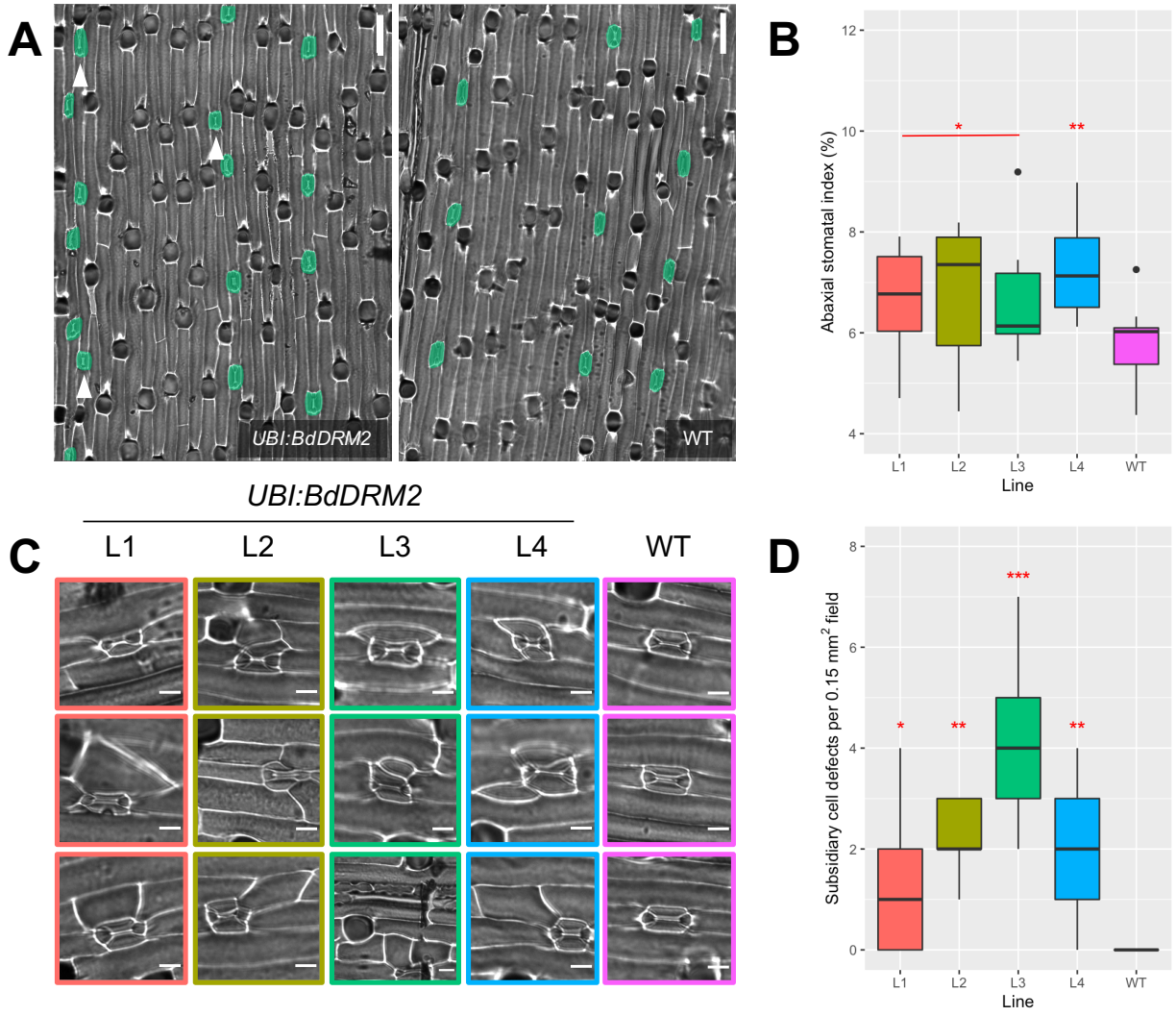

Figure 3.3 *BdDRM2* overexpression alters stomatal index and subsidiary cell development. **(A and C)** Differential interference contrast (DIC) images of *UBI:BdDRM2* and wild-type (Bd21-3) abaxial epidermal imprints. Plants were grown at 22°C under a 16h photoperiod. Images show abaxial surface of third, fully expanded leaf at 18 DPG. **(A)** Stomata are false-coloured green and stomata occurring in hair cell files are indicated by white arrowheads. Prominent dark cells are hair cells. Scale bars: 50 µm. **(B and D)** DIC images of three biological replicates per line were analyzed using Fiji ImageJ. For each biological replicate, three regions of the leaf midsection (~2 cm distal and proximal of leaf collar and leaf tip, respectively) were imaged. **(B)** Abaxial SI, calculated as the percent stomata of total epidermal cells plus stomata, is shown for *UBI:BdDRM2* lines and wild-type (Bd21-3). *P<0.05; **P<0.002 **(C)** SC defects of *UBI:BdDRM2* lines compared to wild-type (Bd21-3). Scale bars: 10 µm. **(D)** SC defects were counted on Fiji ImageJ. The distribution of SC defects was non-normal, as determined by the Shapiro-Wilk test, therefore a Kruskal-Wallis test (nonparametric analog of ANOVA), followed by a Dunn's Multiple Comparisons test was performed to assess significance. *P<0.02; **P<0.001; ***P<0.0001.

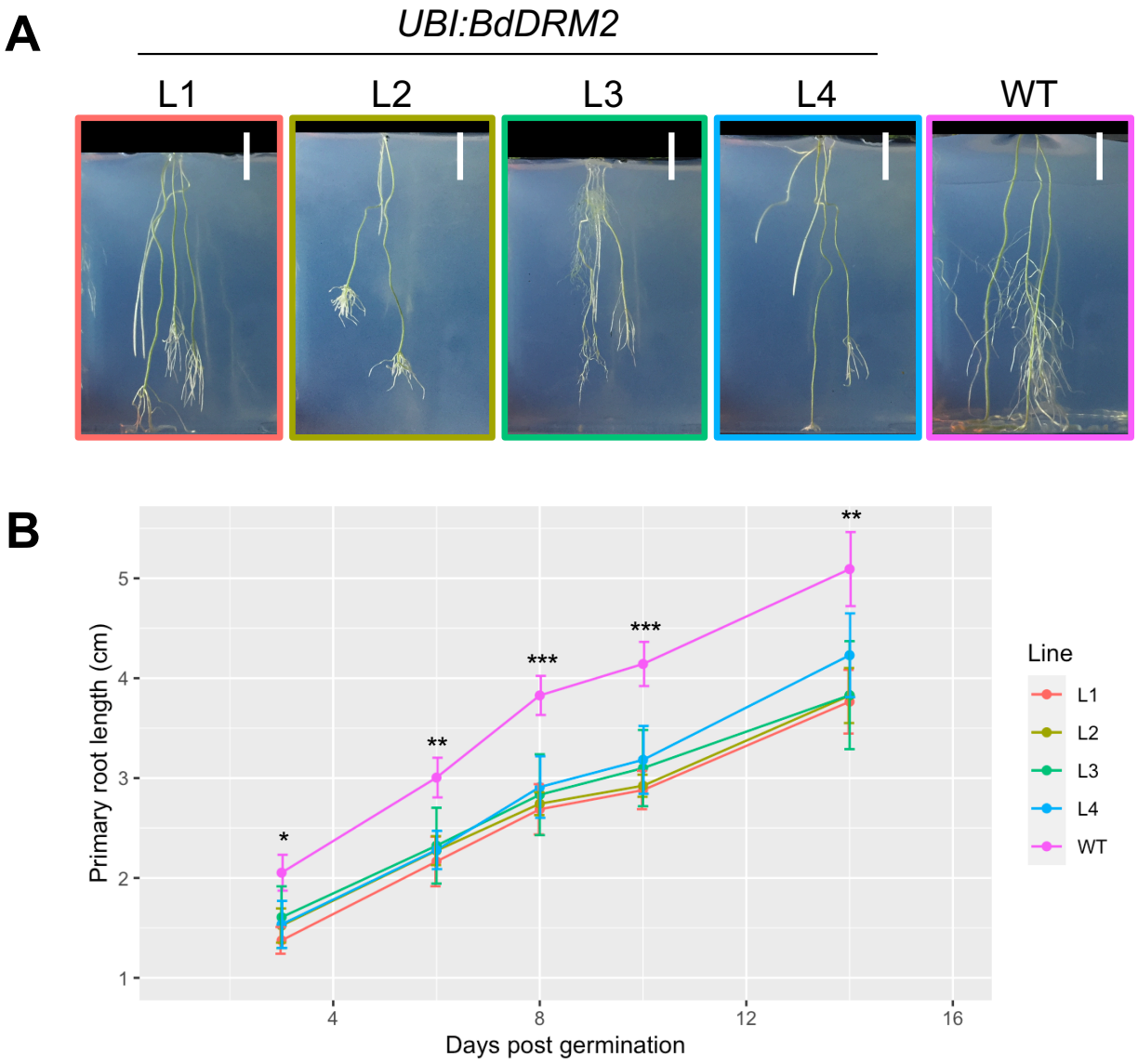

Figure 3.4 *BdDRM2* overexpression inhibits root growth. (A) Phenotype of *UBI:BdDRM2* and wild-type (Bd21-3) roots at 31 DPG. Seeds were sterilized prior to stratification in the dark at 4°C for 7 days to ensure uniform germination. After stratification, seeds were sown on full-strength MS media with 1% Phytagel in specialized root growth chambers (RGCs) designed to allow sterile growth of *B. distachyon* roots for imaging while minimizing root exposure to light (**Supplementary Figure 3.1**). RGCs were randomly distributed in environmental growth chambers set to 22°C with a 16h photoperiod. Root growth was monitored by imaging every 2-3 days for 38 days and RGCs were rotated in growth chambers after imaging to minimize chamber effects. Scale bar: 1 cm. **(B)** Growth rate of *UBI:BdDRM2* and wild-type (Bd21-3) primary root over 14 days. Plot shows the average of four biological replicates ± 1 SD. **P*<0.02; ***P*<0.01; ****P*<0.001.

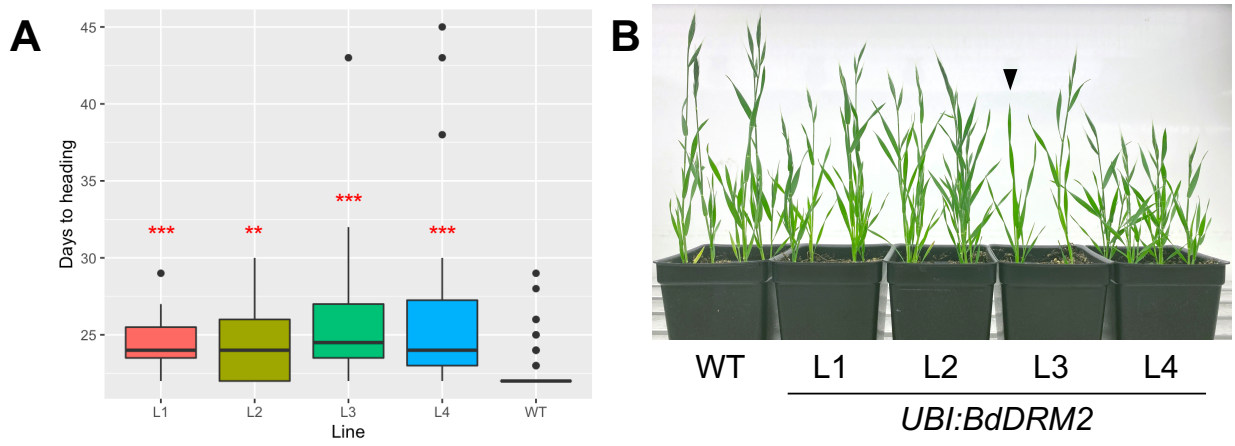

Figure 3.5 *BdDRM2* overexpression delays flowering. (A) Flowering, as measured by days to heading (Zadok's 49), is delayed in *UBI:BdDRM2* lines compared to wild-type (Bd21-3). Plants were vernalized as seed for 14 days at 4°C under a short day 8h photoperiod before being transferred to 22°C under a long day 16h photoperiod. A total of 28 biological replicates (four plants per pot) were observed for each line. Some *UBI:BdDRM2* Line 2 (n = 2) and Line 3 (n = 2) individuals did not flower throughout the course of the experiment. The distribution of days to heading was non-normal, as determined by the Shapiro-Wilk test, therefore a Kruskal-Wallis test (nonparametric analog of ANOVA), followed by a Dunn's Multiple Comparisons test was performed to assess significance. $^{**}P<0.0005$; $^{***}P<0.0001$. **(B)** Phenotype of 35 DPG wild-type (Bd21-3) and *UBI:BdDRM2* lines at flowering. The earlier flowering wild-type plants pictured show uniformly swollen spikes as grain filling proceeds (~ Zadok's 77-85), where *UBI:BdDRM2* development is comparatively delayed at late anthesis to early grain filling (~Zadok's 69-73). Black arrowhead indicates *UBI:BdDRM2* Line 3 individual with flag leaf not yet emerged (prior to Zadok's 37).

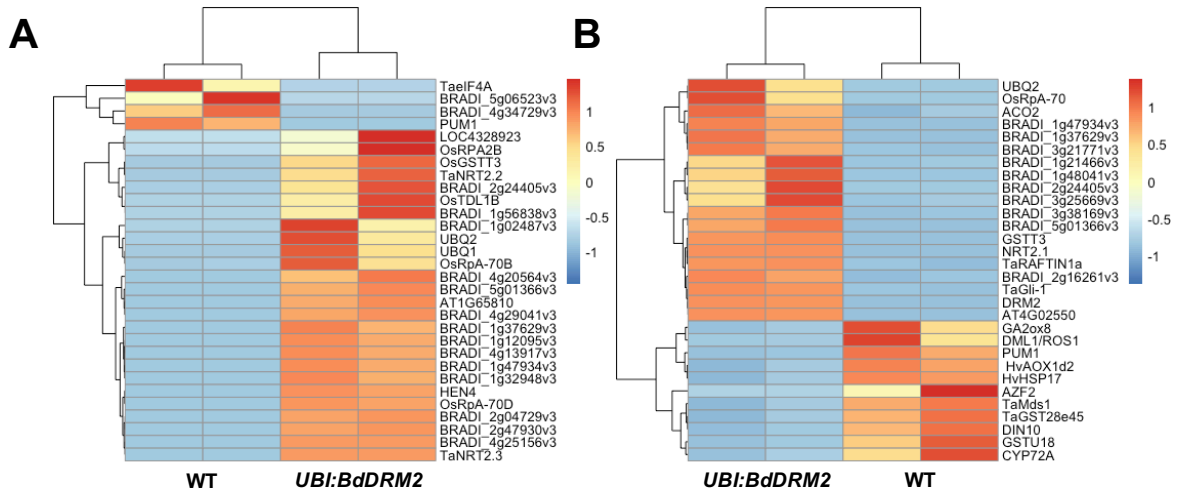

C

Enriched Category	FDR < 0.1 filtered p-value	GOID	Term	Ontology	Definition	Synonym
1	5.84724059392803e-06	GO:0004364	glutathione transferase activity	MF	Catalysis of the reaction: R-X + glutathione = H-X + R-S-glutathione. R may be an aliphatic, aromatic or heterocyclic group; X may be a sulfate, nitrile or halide group.	glutathione conjugation reaction
2	7.28064318634509e-06	GO:0006749	glutathione metabolic process	BP	The chemical reactions and pathways involving glutathione, the tripeptide glutamylcysteinylglycine, which acts as a coenzyme for some enzymes and as an antioxidant in the protection of sulfhydryl groups in enzymes and other proteins; it has a specific role in the reduction of hydrogen peroxide (H2O2) and oxidized ascorbate, and it participates in the gamma-glutamyl cycle.	oxidized glutathione reduction
3	3.60645411187748e-05	GO:0032196	transposition	BP	Any process involved in mediating the movement of discrete segments of DNA between nonhomologous sites.	NA

Figure 3.6 *BdDRM2* overexpression in Bd21-3 background alters the transcriptome. RNA-seq was performed on two biological replicates (each composed of three pooled eight DPG whole seedlings) of *UBI:BdDRM2* (Line 3) and wild-type (Bd21-3) grown at 22°C, 16h photoperiod, sampled mid-photoperiod. Illumina reads were mapped to the Bd21 reference genome (v3.0) using the GenPipes RNA-seq pipeline on Compute Canada cluster resources. Differentially expressed genes (DEGs) were identified through Deseq and edgeR, and further filtered by FDR adjusted *P* values < 0.05 and $|\log_2(\text{fold change})| > 1.5$. A total of 266 DEGs were identified, with 150 and 116 genes respectively upregulated and downregulated in *UBI:BdDRM2* Line 3. Heatmaps show DEGs organized by top 30 largest $|\log_2(\text{fold change})|$ **(A)** and top 30 lowest FDR adjusted *P* values **(B)**. Gene names at right are best hit Nucleotide BLAST results of *B. distachyon* sequences used as queries against *Arabidopsis thaliana* (no prefix), *Triticum aestivum* (Ta), *Hordeum vulgare* (Hv) and *Oryza sativa* (Os) genomes. Where no significant BLAST hits were found or hits in queried genomes were uncharacterized, Brachypodium_distachyon_v3.0 gene IDs were given. Expression data scaled by row z-score. **(C)** Gene ontology (GO) analysis of DEG results (FDR adjusted *P* value < 0.1) conducted via GO-seq. Left to right: first column, ID of category enriched; second column, FDR adjusted *P* value of category enrichment; third column, GO ID; fourth column, term associated with GO ID; fifth column, ontology that term belongs to, either cellular component (CC), biological process (BP) or molecular function (MF); sixth column, definition of term; seventh column, closely related or alternative phrases for term.

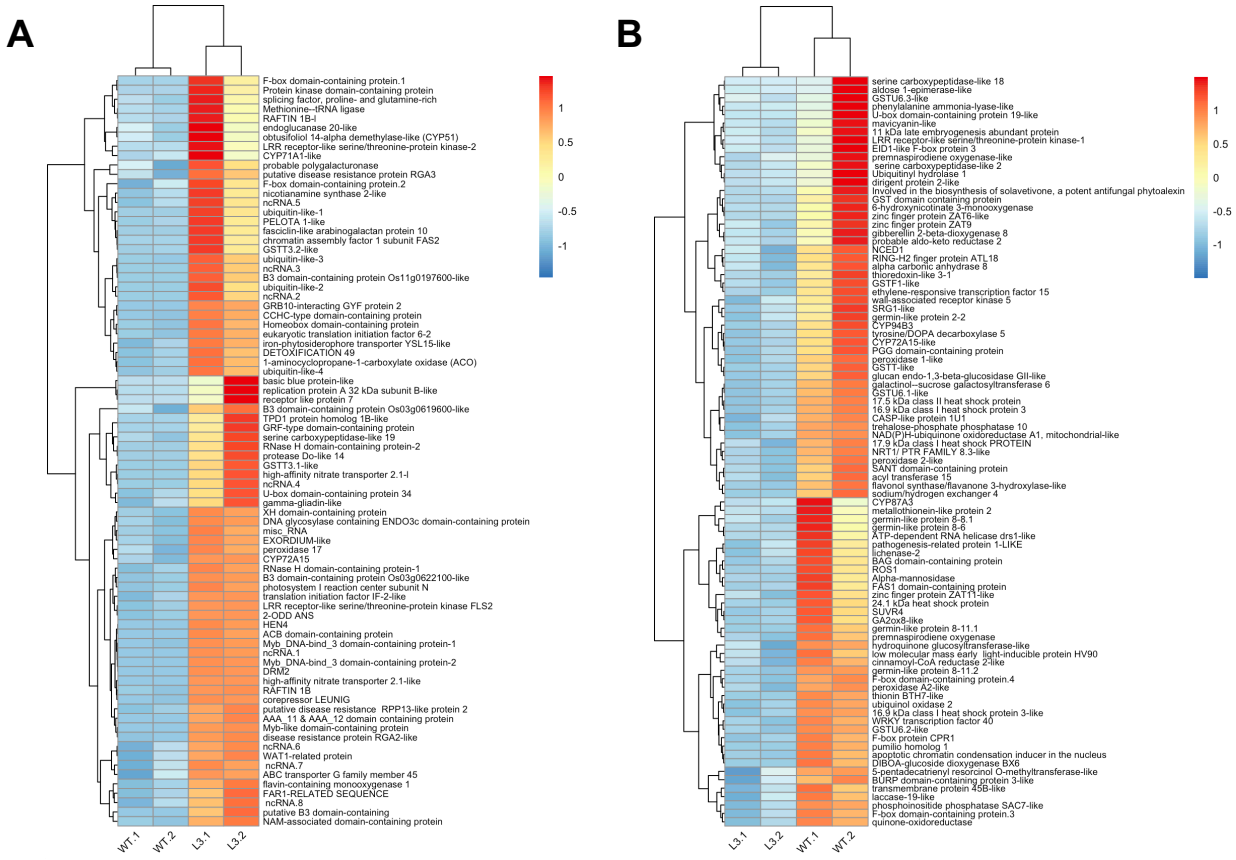

Figure 3.7 Future targets identified by annotated list of DEGs in *UBI:BdDRM2* Line 3. The full filtered (FDR adjusted *P* values < 0.05; $|\log_2(\text{fold change})| > 1.5$) list of differentially expressed genes (DEGs) identified through Deseq and edgeR analyses was searched through EnsemblPlants Brachypodium_distachyon_v3.0 resources for annotation. Each DEG v3.0 gene ID was called on to pull locus definitions or recommended protein names from NCBI RefSeq or UniProtKB databases, respectively. DEG gene IDs where both NCBI and UniProtKB annotations were uncharacterized were excluded from the above heatmaps. Heatmaps showing annotated **(A)** upregulated and downregulated **(B)** genes in *UBI:BdDRM2* Line 3 (biological replicates L3.1 and L3.2) compared to Bd21-3 (biological replicates WT.1 and WT.2). Expression data shown is scaled by row z-score.

CHAPTER IV: CONCLUSIONS

4.1 General conclusions

We hypothesized that the *B. distachyon* DRM homologue, BdDRM2, controls *de novo* DNA methylation in the model grass and the findings of this study have provided evidence in support of this. Notably, we validated our *UBI:BdDRM2* transgenic lines through genomic sequencing and RT-qPCR, and demonstrated that overexpression of *BdDRM2* in *B. distachyon* resulted in genomic hypermethylation.

We also hypothesized that DNA methylation is an important component of gene expression control and the normal growth and development of *B. distachyon*. The results of our transcriptomic analysis of *UBI:BdDRM2* Line 3 indeed provides supportive evidence, as *BdDRM2*-overexpression resulted in an altered transcriptome compared to wild-type, with notable changes in expression to genes involved in glutathione metabolism and transposition. Our phenotypic analysis of the *UBI:BdDRM2* lines provides evidence in support of DNA methylation as a regulator of wild-type growth and developmental patterns, as abnormal stomatal, root growth and flowering time phenotypes were identified in the overexpression mutants.

4.2 Contributions to science

- By completing Objectives 1 and 3, this study has demonstrated the importance of the epigenetic contribution to phenotype in the model cereal, *B. distachyon*, especially for agronomically relevant traits implicated in water use efficiency and yield.
- This study has also identified and characterized the tissue-specific transcription of putative DNA methyltransferases in *B. distachyon* utilizing publicly available resources, which

complements the results of Objective 1 and furthers our knowledge of genome regulation in grasses.

- Furthermore, completion of Objectives 1-3 has provided strong evidence in favour of *BdDRM2* as a conserved *de novo* DNA methyltransferase in *B. distachyon* with biological relevance. The validation and characterization of *UBI:BdDRM2* transgenic lines allows their use for future investigations into the role of DNA methylation in abiotic stress tolerance, which is a particular focus of our lab.
- Finally, completion of Objective 2 has provided a wealth of targets for future investigations into understanding the role of DNA methylation in *B. distachyon*. These targets include (but are not limited to) two DNA demethylase homologs, various hormone metabolic genes, non-coding RNAs implicated in gene silencing, plant developmental transcription factors and a subset of heat shock proteins that may be targeted by RdDM. Future investigations into these findings will be conducted as of January 2021 with the start of Luc Ouellette's PhD project.

4.3 Future directions

Characterization of the *UBI:BdDRM2* transgenic insertions, has informed us that two of our four lines (Lines 1 and 3) have single transgene copies, where the other two (Lines 2 and 4) each have double copies of the transgene (**Figure 3.2A-B**). With this knowledge, we can cross Lines 2 and 4 with non-transgenic Bd21-3 to obtain single-copy, independent lines. Furthermore, because the precise genomic coordinates were obtained in our analyses, specific primers can be designed for each transgenic event to quickly verify the results of crosses.

The analyses conducted herein necessitate the development of *BdDRM2* knockdown or knockout lines to further inform us of the true extent of the *de novo* DNA methyltransferase's role in *B. distachyon*. A major limitation of using overexpression lines is that any observed effects could be artifacts of unnaturally high rates of gene transcription. Therefore, an important next step is to target the *BdDRM2* loci through RNAi-mediated knockdown, or preferably, through CRISPR-Cas9-mediated knockout.

A major limitation of the present study is the current lack of site-specific DNA methylation analyses. We have demonstrated that the *BdDRM2* overexpression lines used in this study accumulate a higher degree of global DNA methylation compared to wild-type, however, the impact of DNA methylation has been observed to be highly-sequence and context-dependent (Lei et al., 2015). Therefore, the next logical step is to take the targets identified in this study and perform sequence-specific DNA methylation analyses via Methylated DNA Immunoprecipitation (MeDIP) or high-throughput bisulfite sequencing.

Recently, a sequence-specific tool (SunTag) for targeted DNA methylation and demethylation activities has been developed in *A. thaliana* (Papikian, Liu, Gallego-Bartolomé, & Jacobsen, 2019). Development of such a tool in *B. distachyon* is feasible due to its ease of transformation and would complement the existing tools in our laboratory. The impact of promoter and/or gene-body DNA methylation on gene expression is largely unclear. These sequence-specific tools will revolutionize DNA methylation analyses in plants by allowing us to target specific genes and even specific regions within genes. Finally, development of the SunTag tool in *B. distachyon* will be a first step towards broader adoption in cereals, opening the door for epigenome engineering in crops.

REFERENCES

Agarwal, P. K., Agarwal, P., Reddy, M. K., & Sopory, S. K. (2006). Role of DREB transcription factors in abiotic and biotic stress tolerance in plants. *Plant Cell Reports*, *25*(12), 1263–1274. https://doi.org/10.1007/s00299-006-0204-8

Aina, R., Sgorbati, S., Santagostino, A., Labra, M., Ghiani, A., & Citterio, S. (2004). Specific hypomethylation of DNA is induced by heavy metals in white clover and industrial hemp. *Physiologia Plantarum*. https://doi.org/10.1111/j.1399-3054.2004.00343.x

Akimoto, K., Katakami, H., Kim, H. J., Ogawa, E., Sano, C. M., Wada, Y., & Sano, H. (2007). Epigenetic inheritance in rice plants. *Annals of Botany*. https://doi.org/10.1093/aob/mcm110

Baniwal, S. K., Bharti, K., Chan, K. Y., Fauth, M., Ganguli, A., Kotak, S., … Zielinski, D. (2004). Heat stress response in plants: A complex game with chaperones and more than twenty heat stress transcription factors. *Journal of Biosciences*. https://doi.org/10.1007/BF02712120

Bannister, A. J., & Kouzarides, T. (2011). Regulation of chromatin by histone modifications. *Cell Research*. https://doi.org/10.1038/cr.2011.22

Bastow, R., Mylne, J. S., Lister, C., Lippman, Z., Martienssen, R. A., & Dean, C. (2004). Vernalization requires epigenetic silencing of FLC by histone methylation. *Nature*. https://doi.org/10.1038/nature02269

Baubec, T., Finke, A., Mittelsten Scheid, O., & Pecinka, A. (2014). Meristem-specific expression of epigenetic regulators safeguards transposon silencing in Arabidopsis. *EMBO Reports*. https://doi.org/10.1002/embr.201337915

Berger, S. L. (2007). The complex language of chromatin regulation during transcription. *Nature*. https://doi.org/10.1038/nature05915

Bernstein, B. E., Mikkelsen, T. S., Xie, X., Kamal, M., Huebert, D. J., Cuff, J., … Lander, E. S. (2006). A Bivalent Chromatin Structure Marks Key Developmental Genes in Embryonic Stem Cells. *Cell*. https://doi.org/10.1016/j.cell.2006.02.041

Berr, A., Shafiq, S., & Shen, W. H. (2011). Histone modifications in transcriptional activation during plant development. *Biochimica et Biophysica Acta - Gene Regulatory Mechanisms*. https://doi.org/10.1016/j.bbagrm.2011.07.001

Bharti, K., Schmidt, E., Lyck, R., Heerklotz, D., Bublak, D., & Scharf, K. D. (2000). Isolation and characterization of HsfA3, a new heat stress transcription factor of Lycopersicon peruvianum. *Plant Journal*. https://doi.org/10.1046/j.1365-313X.2000.00746.x

Bostick, M., Jong, K. K., Estève, P. O., Clark, A., Pradhan, S., & Jacobsen, S. E. (2007). UHRF1 plays a role in maintaining DNA methylation in mammalian cells. *Science*. https://doi.org/10.1126/science.1147939

Bourgey, M., Dali, R., Eveleigh, R., Chen, K. C., Letourneau, L., Fillon, J., … Bourque, G. (2018). GenPipes: an open-source framework for distributed and scalable genomic analyses. *BioRxiv*. https://doi.org/10.1101/459552

Boyko, A., Blevins, T., Yao, Y., Golubov, A., Bilichak, A., Ilnytskyy, Y., … Kovalchuk, I. (2010). Transgenerational adaptation of Arabidopsis to stress requires DNA methylation and the function of dicer-like proteins. *PLoS ONE*. https://doi.org/10.1371/journal.pone.0009514

Bragg, J. N., Wu, J., Gordon, S. P., Guttman, M. E., Thilmony, R., Lazo, G. R., … Vogel, J. P. (2012). Generation and Characterization of the Western Regional Research Center Brachypodium T-DNA Insertional Mutant Collection. *PLoS ONE*.

https://doi.org/10.1371/journal.pone.0041916
Candaele, J., Demuynck, K., Mosoti, D., Beemster, G. T. S., Inze, D., & Nelissen, H. (2014). Differential Methylation during Maize Leaf Growth Targets Developmentally Regulated Genes. *PLANT PHYSIOLOGY*. https://doi.org/10.1104/pp.113.233312
Cao, X., Aufsatz, W., Zilberman, D., Mette, M. F., Huang, M. S., Matzke, M., & Jacobsen, S. E. (2003). Role of the DRM and CMT3 Methyltransferases in RNA-Directed DNA Methylation. *Current Biology*, *13*(24), 2212–2217. https://doi.org/10.1016/j.cub.2003.11.052
Cao, X., & Jacobsen, S. E. (2002a). Locus-specific control of asymmetric and CpNpG methylation by the DRM and CMT3 methyltransferase genes. *Proceedings of the National Academy of Sciences*. https://doi.org/10.1073/pnas.162371599
Cao, X., & Jacobsen, S. E. (2002b). Role of the Arabidopsis DRM methyltransferases in de novo DNA methylation and gene silencing. *Current Biology*. https://doi.org/10.1016/S0960-9822(02)00925-9
Cao, X., Springer, N. M., Muszynski, M. G., Phillips, R. L., Kaeppler, S., & Jacobsen, S. E. (2000). Conserved plant genes with similarity to mammalian de novo DNA methyltransferases. *Proceedings of the National Academy of Sciences*. https://doi.org/10.1073/pnas.97.9.4979
Casadesus, J., & Low, D. (2006). Epigenetic Gene Regulation in the Bacterial World. *Microbiology and Molecular Biology Reviews*. https://doi.org/10.1128/MMBR.00016-06
Chan, S. W. L., Henderson, I. R., Zhang, X., Shah, G., Chien, J. S. C., & Jacobsen, S. E. (2006). RNAi, DRD1, and histone methylation actively target developmentally important Non-CG DNA methylation in Arabidopsis. *PLoS Genetics*. https://doi.org/10.1371/journal.pgen.0020083
Chinnusamy, V., & Zhu, J. K. (2009). Epigenetic regulation of stress responses in plants. *Current Opinion in Plant Biology*. https://doi.org/10.1016/j.pbi.2008.12.006
Cokus, S. J., Feng, S., Zhang, X., Chen, Z., Merriman, B., Haudenschild, C. D., … Jacobsen, S. E. (2008). Shotgun bisulphite sequencing of the Arabidopsis genome reveals DNA methylation patterning. *Nature*. https://doi.org/10.1038/nature06745
Cubas, P., Vincent, C., & Coen, E. (1999). An epigenetic mutation responsible for natural variation in floral symmetry. *Nature*. https://doi.org/10.1038/43657
Dangwal, M., Malik, G., Kapoor, S., & Kapoor, M. (2013). De novo methyltransferase, OsDRM2, interacts with the ATP-dependent RNA helicase, OseIF4A, in rice. *Journal of Molecular Biology*. https://doi.org/10.1016/j.jmb.2013.05.021
Davidson, R. M., Gowda, M., Moghe, G., Lin, H., Vaillancourt, B., Shiu, S. H., … Robin Buell, C. (2012). Comparative transcriptomics of three Poaceae species reveals patterns of gene expression evolution. *Plant Journal*. https://doi.org/10.1111/j.1365-313X.2012.05005.x
Devaiah, B. N., Nagarajan, V. K., & Raghothama, K. G. (2007). Phosphate homeostasis and root development in arabidopsis are synchronized by the zinc finger transcription factor ZAT6. *Plant Physiology*. https://doi.org/10.1104/pp.107.101691
Dowen, R. H., Pelizzola, M., Schmitz, R. J., Lister, R., Dowen, J. M., Nery, J. R., … Ecker, J. R. (2012). Widespread dynamic DNA methylation in response to biotic stress. *Proceedings of the National Academy of Sciences*. https://doi.org/10.1073/pnas.1209329109
Draper, J. (2001). Brachypodium distachyon. A New Model System for Functional Genomics in Grasses. *PLANT PHYSIOLOGY*. https://doi.org/10.1104/pp.127.4.1539
Du, J., Zhong, X., Bernatavichute, Y. V., Stroud, H., Feng, S., Caro, E., … Jacobsen, S. E.

(2012). Dual binding of chromomethylase domains to H3K9me2-containing nucleosomes directs DNA methylation in plants. *Cell*. https://doi.org/10.1016/j.cell.2012.07.034
Durand, S., Bouché, N., Perez Strand, E., Loudet, O., & Camilleri, C. (2012). Rapid establishment of genetic incompatibility through natural epigenetic variation. *Current Biology*. https://doi.org/10.1016/j.cub.2011.12.054
Dyachenko, O. V., Zakharchenko, N. S., Shevchuk, T. V., Bohnert, H. J., Cushman, J. C., & Buryanov, Y. I. (2006). Effect of hypermethylation of CCWGG sequences in DNA of Mesembryanthemum crystallinum plants on their adaptation to salt stress. *Biochemistry (Moscow)*. https://doi.org/10.1134/S000629790604016X
Furner, I. J., & Matzke, M. (2011). Methylation and demethylation of the Arabidopsis genome. *Current Opinion in Plant Biology*. https://doi.org/10.1016/j.pbi.2010.11.004
Galaud, J. -P, Gaspar, T., & Boyer, N. (1993). Inhibition of internode growth due to mechanical stress in Bryonia dioica: relationship between changes in DNA methylation and ethylene metabolism. *Physiologia Plantarum*. https://doi.org/10.1111/j.1399-3054.1993.tb08786.x
Gao, G., Li, J., Li, H., Li, F., Xu, K., Yan, G., … Wu, X. (2014). Comparison of the heat stress induced variations in DNA methylation between heat-tolerant and heat-sensitive rapeseed seedlings. *Breeding Science*. https://doi.org/10.1270/jsbbs.64.125
García-Giménez, J. L., Romá-Mateo, C., Pérez-Machado, G., Peiró-Chova, L., & Pallardó, F. V. (2017). Role of glutathione in the regulation of epigenetic mechanisms in disease. *Free Radical Biology and Medicine*. https://doi.org/10.1016/j.freeradbiomed.2017.07.008
Gehring, M., Bubb, K. L., & Henikoff, S. (2009). Extensive demethylation of repetitive elements during seed development underlies gene imprinting. *Science*. https://doi.org/10.1126/science.1171609
Golldack, D., Lüking, I., & Yang, O. (2011). Plant tolerance to drought and salinity: Stress regulating transcription factors and their functional significance in the cellular transcriptional network. *Plant Cell Reports*. https://doi.org/10.1007/s00299-011-1068-0
Gordon, S. P., Contreras-Moreira, B., Woods, D. P., Des Marais, D. L., Burgess, D., Shu, S., … Vogel, J. P. (2017). Extensive gene content variation in the Brachypodium distachyon pan-genome correlates with population structure. *Nature Communications*. https://doi.org/10.1038/s41467-017-02292-8
Grigoryev, S. A. (2012). Nucleosome spacing and chromatin higher-order folding. *Nucleus (United States)*. https://doi.org/10.4161/nucl.22168
Guertin, M. J., & Lis, J. T. (2010). Chromatin landscape dictates HSF binding to target DNA elements. *PLoS Genetics*. https://doi.org/10.1371/journal.pgen.1001114
Guo, M., Liu, J.-H., Ma, X., Luo, D.-X., Gong, Z.-H., & Lu, M.-H. (2016). The Plant Heat Stress Transcription Factors (HSFs): Structure, Regulation, and Function in Response to Abiotic Stresses. *Frontiers in Plant Science*. https://doi.org/10.3389/fpls.2016.00114
Guo, M., Lu, J. P., Zhai, Y. F., Chai, W. G., Gong, Z. H., & Lu, M. H. (2015). Genome-wide analysis, expression profile of heat shock factor gene family (CaHsfs) and characterisation of CaHsfA2 in pepper (Capsicum annuum L.). *BMC Plant Biology*. https://doi.org/10.1186/s12870-015-0512-7
Guzy-Wrobelska, J., Filek, M., Kaliciak, A., Szarejko, I., Macháčková, I., Krekule, J., & Barciszewska, M. (2013). Vernalization and photoperiod-related changes in the DNA methylation state in winter and spring rapeseed. *Acta Physiologiae Plantarum*. https://doi.org/10.1007/s11738-012-1126-4
Haag, J. R., & Pikaard, C. S. (2011). Multisubunit RNA polymerases IV and V: Purveyors of

non-coding RNA for plant gene silencing. *Nature Reviews Molecular Cell Biology*. https://doi.org/10.1038/nrm3152

Hanin, M., Brini, F., Ebel, C., Toda, Y., Takeda, S., & Masmoudi, K. (2011). Plant dehydrins and stress tolerance: versatile proteins for complex mechanisms. *Plant Signal Behav*. https://doi.org/10.4161/psb.6.10.17088

Harris, C. J., Scheibe, M., Wongpalee, S. P., Liu, W., Cornett, E. M., Vaughan, R. M., … Jacobsen, S. E. (2018). A DNA methylation reader complex that enhances gene transcription. *Science*, *362*(6419), 1182–1186. https://doi.org/10.1126/science.aar7854

He, L., Wu, W., Zinta, G., Yang, L., Wang, D., Liu, R., … Zhu, J. K. (2018). A naturally occurring epiallele associates with leaf senescence and local climate adaptation in Arabidopsis accessions. *Nature Communications*. https://doi.org/10.1038/s41467-018-02839-3

He, X. J., Chen, T., & Zhu, J. K. (2011). Regulation and function of DNA methylation in plants and animals. *Cell Research*. https://doi.org/10.1038/cr.2011.23

Henderson, I. R., Deleris, A., Wong, W., Zhong, X., Chin, H. G., Horwitz, G. A., … Jacobsen, S. E. (2010). The De novo cytosine methyltransferase DRM2 requires intact UBA domains and a catalytically mutated paralog DRM3 during RNA-directed DNA methylation in arabidopsis thaliana. *PLoS Genetics*. https://doi.org/10.1371/journal.pgen.1001182

Henderson, I. R., & Jacobsen, S. E. (2007). Epigenetic inheritance in plants. *Nature*, *447*, 418. Retrieved from https://doi.org/10.1038/nature05917

Hergeth, S. P., & Schneider, R. (2015). The H1 linker histones: multifunctional proteins beyond the nucleosomal core particle. *EMBO Reports*. https://doi.org/10.15252/embr.201540749

Hollister, J. D., & Gaut, B. S. (2009). Epigenetic silencing of transposable elements: A trade-off between reduced transposition and deleterious effects on neighboring gene expression. *Genome Research*. https://doi.org/10.1101/gr.091678.109

Hong, S. Y., Seo, P. J., Yang, M. S., Xiang, F., & Park, C. M. (2008). Exploring valid reference genes for gene expression studies in Brachypodium distachyon by real-time PCR. *BMC Plant Biology*. https://doi.org/10.1186/1471-2229-8-112

Houben, M., & Van de Poel, B. (2019). 1-aminocyclopropane-1-carboxylic acid oxidase (ACO): The enzyme that makes the plant hormone ethylene. *Frontiers in Plant Science*. https://doi.org/10.3389/fpls.2019.00695

Hsia, M. M., O'Malley, R., Cartwright, A., Nieu, R., Gordon, S. P., Kelly, S., … Vogel, J. P. (2017). Sequencing and functional validation of the JGI Brachypodium distachyon T-DNA collection. *Plant Journal*. https://doi.org/10.1111/tpj.13582

Hsieh, T. F., Ibarra, C. A., Silva, P., Zemach, A., Eshed-Williams, L., Fischer, R. L., & Zilberman, D. (2009). Genome-wide demethylation of Arabidopsis endosperm. *Science*. https://doi.org/10.1126/science.1172417

Huan, Q., Mao, Z., Chong, K., & Zhang, J. (2018). Global analysis of H3K4me3/H3K27me3 in Brachypodium distachyon reveals VRN3 as critical epigenetic regulation point in vernalization and provides insights into epigenetic memory. *New Phytologist*. https://doi.org/10.1111/nph.15288

Huh, J. H., Bauer, M. J., Hsieh, T. F., & Fischer, R. L. (2008). Cellular Programming of Plant Gene Imprinting. *Cell*. https://doi.org/10.1016/j.cell.2008.02.018

Hye, R. W., Pontes, O., Pikaard, C. S., & Richards, E. J. (2007). VIM1, a methylcytosine-binding protein required for centromeric heterochromatinization. *Genes and Development*. https://doi.org/10.1101/gad.1512007

Ibarra, C. A., Feng, X., Schoft, V. K., Hsieh, T. F., Uzawa, R., Rodrigues, J. A., … Zilberman, D. (2012). Active DNA demethylation in plant companion cells reinforces transposon methylation in gametes. *Science*. https://doi.org/10.1126/science.1224839

Ito, H., Gaubert, H., Bucher, E., Mirouze, M., Vaillant, I., & Paszkowski, J. (2011). An siRNA pathway prevents transgenerational retrotransposition in plants subjected to stress. *Nature*. https://doi.org/10.1038/nature09861

Jenuwein, T., & Allis, C. D. (2001). Translating the histone code. *Science*. https://doi.org/10.1126/science.1063127

Jin, B., Li, Y., & Robertson, K. D. (2011). DNA methylation: Superior or subordinate in the epigenetic hierarchy? *Genes and Cancer*. https://doi.org/10.1177/1947601910393957

Joly-Lopez, Z., & Bureau, T. E. (2014). Diversity and evolution of transposable elements in Arabidopsis. *Chromosome Research*. https://doi.org/10.1007/s10577-014-9418-8

Jullien, P. E., Susaki, D., Yelagandula, R., Higashiyama, T., & Berger, F. (2012). DNA methylation dynamics during sexual reproduction in Arabidopsis thaliana. *Current Biology*. https://doi.org/10.1016/j.cub.2012.07.061

Kankel, M. W., Ramsey, D. E., Stokes, T. L., Flowers, S. K., Haag, J. R., Jeddeloh, J. A., … Richards, E. J. (2003). Arabidopsis MET1 cytosine methyltransferase mutants. *Genetics*.

Kawakatsu, T., Huang, S. shan C., Jupe, F., Sasaki, E., Schmitz, R. J. J., Urich, M. A. A., … Ecker, J. R. (2016). Epigenomic Diversity in a Global Collection of Arabidopsis thaliana Accessions. *Cell*. https://doi.org/10.1016/j.cell.2016.06.044

Kawakatsu, T., Nery, J. R., Castanon, R., & Ecker, J. R. (2017). Dynamic DNA methylation reconfiguration during seed development and germination. *Genome Biology*. https://doi.org/10.1186/s13059-017-1251-x

Khan, A. R., Enjalbert, J., Marsollier, A. C., Rousselet, A., Goldringer, I., & Vitte, C. (2013). Vernalization treatment induces site-specific DNA hypermethylation at the VERNALIZATION-A1 (VRN-A1) locus in hexaploid winter wheat. *BMC Plant Biology*. https://doi.org/10.1186/1471-2229-13-209

Kinoshita, T. (1999). Imprinting of the MEDEA Polycomb Gene in the Arabidopsis Endosperm. *THE PLANT CELL ONLINE*. https://doi.org/10.1105/tpc.11.10.1945

Kornberg, R. D., & Lorch, Y. (1999). Twenty-five years of the nucleosome, fundamental particle of the eukaryote chromosome. *Cell*. https://doi.org/10.1016/S0092-8674(00)81958-3

Kotak, S., Larkindale, J., Lee, U., von Koskull-Döring, P., Vierling, E., & Scharf, K. D. (2007). Complexity of the heat stress response in plants. *Current Opinion in Plant Biology*. https://doi.org/10.1016/j.pbi.2007.04.011

Kou, H. P., Li, Y., Song, X. X., Ou, X. F., Xing, S. C., Ma, J., … Liu, B. (2011). Heritable alteration in DNA methylation induced by nitrogen-deficiency stress accompanies enhanced tolerance by progenies to the stress in rice (Oryza sativa L.). *Journal of Plant Physiology*. https://doi.org/10.1016/j.jplph.2011.03.017

Krause, K., & Turck, F. (2018). Plant H3K27me3 has finally found its readers. *Nature Genetics*. https://doi.org/10.1038/s41588-018-0201-1

Kumar, A., Sharma, S., Chunduri, V., Kaur, A., Kaur, S., Malhotra, N., … Garg, M. (2020). Genome-wide Identification and Characterization of Heat Shock Protein Family Reveals Role in Development and Stress Conditions in Triticum aestivum L. *Scientific Reports*. https://doi.org/10.1038/s41598-020-64746-2

Lamaoui, M., Jemo, M., Datla, R., & Bekkaoui, F. (2018). Heat and Drought Stresses in Crops and Approaches for Their Mitigation. *Frontiers in Chemistry*.

https://doi.org/10.3389/fchem.2018.00026
Lata, C., & Prasad, M. (2011). Role of DREBs in regulation of abiotic stress responses in plants. *Journal of Experimental Botany*. https://doi.org/10.1093/jxb/err210
Latzel, V., Allan, E., Bortolini Silveira, A., Colot, V., Fischer, M., & Bossdorf, O. (2013). Epigenetic diversity increases the productivity and stability of plant populations. *Nature Communications*. https://doi.org/10.1038/ncomms3875
Law, J. A., Du, J., Hale, C. J., Feng, S., Krajewski, K., Palanca, A. M. S., … Jacobsen, S. E. (2013). Polymerase IV occupancy at RNA-directed DNA methylation sites requires SHH1. *Nature*. https://doi.org/10.1038/nature12178
Law, J. A., & Jacobsen, S. E. (2010). Establishing, maintaining and modifying DNA methylation patterns in plants and animals. *Nature Reviews Genetics*. https://doi.org/10.1038/nrg2719
Lawrence, M., Daujat, S., & Schneider, R. (2016). Lateral Thinking: How Histone Modifications Regulate Gene Expression. *Trends in Genetics*. https://doi.org/10.1016/j.tig.2015.10.007
Le, T. N., Schumann, U., Smith, N. A., Tiwari, S., Khang Au, P. C., Zhu, Q. H., … Wang, M. B. (2014). DNA demethylases target promoter transposable elements to positively regulate stress responsive genes in Arabidopsis. *Genome Biology*. https://doi.org/10.1186/s13059-014-0458-3
Lei, M., Zhang, H., Julian, R., Tang, K., Xie, S., & Zhu, J.-K. (2015). Regulatory link between DNA methylation and active demethylation in *Arabidopsis*. *Proceedings of the National Academy of Sciences*. https://doi.org/10.1073/pnas.1502279112
Li, X., Wang, X., He, K., Ma, Y., Su, N., He, H., … Deng, X. W. (2008). High-Resolution Mapping of Epigenetic Modifications of the Rice Genome Uncovers Interplay between DNA Methylation, Histone Methylation, and Gene Expression. *THE PLANT CELL ONLINE*. https://doi.org/10.1105/tpc.107.056879
Li, Y., Kumar, S., & Qian, W. (2018). Active DNA demethylation: mechanism and role in plant development. *Plant Cell Reports*. https://doi.org/10.1007/s00299-017-2215-z
Lippman, Z., Gendrel, A. V., Black, M., Vaughn, M. W., Dedhia, N., McCombie, W. R., … Martienssen, R. (2004). Role of transposable elements in heterochromatin and epigenetic control. *Nature*. https://doi.org/10.1038/nature02651
Little, D. Y., Rao, H., Oliva, S., Daniel-Vedele, F., Krapp, A., & Malamy, J. E. (2005). The putative high-affinity nitrate transporter NRT2.1 represses lateral root initiation in response to nutritional cues. *Proceedings of the National Academy of Sciences of the United States of America*. https://doi.org/10.1073/pnas.0504219102
Liu, X., Wang, C., Liu, W., Li, J., Li, C., Kou, X., … Gao, S. (2016). Distinct features of H3K4me3 and H3K27me3 chromatin domains in pre-implantation embryos. *Nature*. https://doi.org/10.1038/nature19362
Liu, Z. W., Shao, C. R., Zhang, C. J., Zhou, J. X., Zhang, S. W., Li, L., … He, X. J. (2014). The SET Domain Proteins SUVH2 and SUVH9 Are Required for Pol V Occupancy at RNA-Directed DNA Methylation Loci. *PLoS Genetics*. https://doi.org/10.1371/journal.pgen.1003948
Lorincz, M. C., Dickerson, D. R., Schmitt, M., & Groudine, M. (2004). Intragenic DNA methylation alters chromatin structure and elongation efficiency in mammalian cells. *Nature Structural and Molecular Biology*. https://doi.org/10.1038/nsmb840
Luger, K., Mäder, A. W., Richmond, R. K., Sargent, D. F., & Richmond, T. J. (1997). Crystal structure of the nucleosome core particle at 2.8 Å resolution. *Nature*. https://doi.org/10.1038/38444

Ma, L., & Li, G. (2018). FAR1-RELATED SEQUENCE (FRS) AND FRS-RELATED FACTOR (FRF) family proteins in arabidopsis growth and development. *Frontiers in Plant Science*. https://doi.org/10.3389/fpls.2018.00692

Madeira, F., Park, Y. M., Lee, J., Buso, N., Gur, T., Madhusoodanan, N., … Lopez, R. (2019). The EMBL-EBI search and sequence analysis tools APIs in 2019. *Nucleic Acids Research*. https://doi.org/10.1093/nar/gkz268

Mann, D. G. J., Lafayette, P. R., Abercrombie, L. L., Parrott, W. A., & Stewart, C. N. (2011). pANIC: A Versatile Set of Gateway-Compatible Vectors for Gene Overexpression and RNAi-Mediated down-Regulation in Monocots. In *Plant Transformation Technologies*. https://doi.org/10.1002/9780470958988.ch11

Manning, K., Tör, M., Poole, M., Hong, Y., Thompson, A. J., King, G. J., … Seymour, G. B. (2006). A naturally occurring epigenetic mutation in a gene encoding an SBP-box transcription factor inhibits tomato fruit ripening. *Nature Genetics*. https://doi.org/10.1038/ng1841

Marmorstein, R., & Zhou, M. M. (2014). Writers and readers of histone acetylation: Structure, mechanism, and inhibition. *Cold Spring Harbor Perspectives in Biology*. https://doi.org/10.1101/cshperspect.a018762

Martin, A., Troadec, C., Boualem, A., Rajab, M., Fernandez, R., Morin, H., … Bendahmane, A. (2009). A transposon-induced epigenetic change leads to sex determination in melon. *Nature*. https://doi.org/10.1038/nature08498

Matzke, M. A., & Mosher, R. A. (2014). RNA-directed DNA methylation: An epigenetic pathway of increasing complexity. *Nature Reviews Genetics*. https://doi.org/10.1038/nrg3683

Mayer, B. F., Ali-Benali, M. A., Demone, J., Bertrand, A., & Charron, J. B. (2015). Cold acclimation induces distinctive changes in the chromatin state and transcript levels of COR genes in Cannabis sativa varieties with contrasting cold acclimation capacities. *Physiologia Plantarum*. https://doi.org/10.1111/ppl.12318

Mayer, B. F., Bertrand, A., & Charron, J. B. (2020). Treatment Analogous to Seasonal Change Demonstrates the Integration of Cold Responses in Brachypodium distachyon1[OPEN]. *Plant Physiology*. https://doi.org/10.1104/pp.19.01195

Mayer, B. F., & Charron, J. B. (2020). Transcriptional memories mediate the plasticity of cold stress responses to enable morphological acclimation in Brachypodium distachyon. *New Phytologist*. https://doi.org/10.1111/nph.16945

Michaels, S. D., & Amasino, R. M. (2000). Memories of winter: Vernalization and the competence to flower. *Plant, Cell and Environment*. https://doi.org/10.1046/j.1365-3040.2000.00643.x

Mirouze, M., & Vitte, C. (2014). Transposable elements, a treasure trove to decipher epigenetic variation: insights from Arabidopsis and crop epigenomes. *Journal of Experimental Botany*. https://doi.org/10.1093/jxb/eru120

Miura, K., Agetsuma, M., Kitano, H., Yoshimura, A., Matsuoka, M., Jacobsen, S. E., & Ashikari, M. (2009). A metastable DWARF1 epigenetic mutant affecting plant stature in rice. *Proceedings of the National Academy of Sciences*. https://doi.org/10.1073/pnas.0901942106

Mohapatra, S. S., & Biondi, E. G. (2017). DNA Methylation in Prokaryotes: Regulation and Function. In T. Krell (Ed.), *Cellular Ecophysiology of Microbe* (pp. 1–21). Cham: Springer International Publishing. https://doi.org/10.1007/978-3-319-20796-4_23-1

Moritoh, S., Eun, C. H., Ono, A., Asao, H., Okano, Y., Yamaguchi, K., … Terada, R. (2012). Targeted disruption of an orthologue of DOMAINS REARRANGED METHYLASE 2, OsDRM2, impairs the growth of rice plants by abnormal DNA methylation. *Plant Journal*. https://doi.org/10.1111/j.1365-313X.2012.04974.x

Mull, L., Ebbs, M. L., & Bender, J. (2006). A histone methylation-dependent DNA methylation pathway is uniquely impaired by deficiency in arabidopsis S-adenosylhomocysteine hydrolase. *Genetics*. https://doi.org/10.1534/genetics.106.063974

Mur, L. A. J., Allainguillaume, J., Catalán, P., Hasterok, R., Jenkins, G., Lesniewska, K., … Vogel, J. (2011). Exploiting the brachypodium tool box in cereal and grass research. *New Phytologist*. https://doi.org/10.1111/j.1469-8137.2011.03748.x

Naumann, U., Daxinger, L., Kanno, T., Eun, C., Long, Q., Lorkovic, Z. J., … Matzke, A. J. M. (2011). Genetic evidence that DNA methyltransferase DRM2 has a direct catalytic role in RNA-directed DNA methylation in Arabidopsis thaliana. *Genetics*. https://doi.org/10.1534/genetics.110.125401

Naydenov, M., Baev, V., Apostolova, E., Gospodinova, N., Sablok, G., Gozmanova, M., & Yahubyan, G. (2015). High-temperature effect on genes engaged in DNA methylation and affected by DNA methylation in Arabidopsis. *Plant Physiology and Biochemistry*. https://doi.org/10.1016/j.plaphy.2014.12.022

Okitsu, C. Y., & Hsieh, C.-L. (2007). DNA Methylation Dictates Histone H3K4 Methylation. *Molecular and Cellular Biology*. https://doi.org/10.1128/MCB.02291-06

Ou, X., Zhang, Y., Xu, C., Lin, X., Zang, Q., Zhuang, T., … Liu, B. (2012). Transgenerational Inheritance of Modified DNA Methylation Patterns and Enhanced Tolerance Induced by Heavy Metal Stress in Rice (Oryza sativa L.). *PLoS ONE*. https://doi.org/10.1371/journal.pone.0041143

Pandey, G., Sharma, N., Sahu, P., & Prasad, M. (2016). Chromatin-Based Epigenetic Regulation of Plant Abiotic Stress Response. *Current Genomics*. https://doi.org/10.2174/1389202917666616052010

Papikian, A., Liu, W., Gallego-Bartolomé, J., & Jacobsen, S. E. (2019). Site-specific manipulation of Arabidopsis loci using CRISPR-Cas9 SunTag systems. *Nature Communications*. https://doi.org/10.1038/s41467-019-08736-7

Park, D., Park, S. H., Ban, Y. W., Kim, Y. S., Park, K. C., Kim, N. S., … Choi, I. Y. (2017). A bioinformatics approach for identifying transgene insertion sites using whole genome sequencing data. *BMC Biotechnology*. https://doi.org/10.1186/s12896-017-0386-x

Pavet, V., Quintero, C., Cecchini, N. M., Rosa, A. L., & Alvarez, M. E. (2006). *Arabidopsis* Displays Centromeric DNA Hypomethylation and Cytological Alterations of Heterochromatin Upon Attack by *Pseudomonas syringae*. *Molecular Plant-Microbe Interactions*. https://doi.org/10.1094/MPMI-19-0577

Phukan, U. J., Jeena, G. S., Tripathi, V., & Shukla, R. K. (2017). Regulation of Apetala2/Ethylene response factors in plants. *Frontiers in Plant Science*. https://doi.org/10.3389/fpls.2017.00150

Pillitteri, L. J., Guo, X., & Dong, J. (2016). Asymmetric cell division in plants: mechanisms of symmetry breaking and cell fate determination. *Cellular and Molecular Life Sciences*. https://doi.org/10.1007/s00018-016-2290-2

Pina, C. (2005). Gene Family Analysis of the Arabidopsis Pollen Transcriptome Reveals Biological Implications for Cell Growth, Division Control, and Gene Expression Regulation. *PLANT PHYSIOLOGY*. https://doi.org/10.1104/pp.104.057935

Qian, W., Miki, D., Lei, M., Zhu, X., Zhang, H., Liu, Y., … Zhu, J. K. (2014). Regulation of active DNA Demethylation by an α-crystallin domain protein in arabidopsis. *Molecular Cell*. https://doi.org/10.1016/j.molcel.2014.06.008

Qu, A. L., Ding, Y. F., Jiang, Q., & Zhu, C. (2013). Molecular mechanisms of the plant heat stress response. *Biochemical and Biophysical Research Communications*. https://doi.org/10.1016/j.bbrc.2013.01.104

Quadrana, L., Almeida, J., Asís, R., Duffy, T., Dominguez, P. G., Bermúdez, L., … Carrari, F. (2014). Natural occurring epialleles determine vitamin e accumulation in tomato fruits. *Nature Communications*. https://doi.org/10.1038/ncomms5027

Quadrana, L., Silveira, A. B., Mayhew, G. F., LeBlanc, C., Martienssen, R. A., Jeddeloh, J. A., & Colot, V. (2016). The Arabidopsis thaliana mobilome and its impact at the species level. *ELife*. https://doi.org/10.7554/eLife.15716

R Core Team. (2019). R: A language and environment for statistical computing. Version 3.5.3. *R Foundation for Statistical Computing, Vienna, Austria*.

Radchuk, V. V., Sreenivasulu, N., Radchuk, R. I., Wobus, U., & Weschke, W. (2005). The methylation cycle and its possible functions in barley endosperm development. *Plant Molecular Biology*. https://doi.org/10.1007/s11103-005-8881-1

Raissig, M. T., Abrash, E., Bettadapur, A., Vogel, J. P., & Bergmann, D. C. (2016). Grasses use an alternatively wired bHLH transcription factor network to establish stomatal identity. *Proceedings of the National Academy of Sciences of the United States of America*. https://doi.org/10.1073/pnas.1606728113

Raissig, M. T., Matos, J. L., Gil, M. X. A., Kornfeld, A., Bettadapur, A., Abrash, E., … Bergmann, D. C. (2017). Mobile MUTE specifies subsidiary cells to build physiologically improved grass stomata. *Science*. https://doi.org/10.1126/science.aal3254

Ream, T. S., Woods, D. P., & Amasino, R. M. (2012). The molecular basis of vernalization in different plant groups. *Cold Spring Harbor Symposia on Quantitative Biology*. https://doi.org/10.1101/sqb.2013.77.014449

Robinson, P. J., & Rhodes, D. (2006). Structure of the “30 nm” chromatin fibre: A key role for the linker histone. *Current Opinion in Structural Biology*. https://doi.org/10.1016/j.sbi.2006.05.007

Saleh, A., Al-Abdallat, A., Ndamukong, I., Alvarez-Venegas, R., & Avramova, Z. (2007). The Arabidopsis homologs of trithorax (ATX1) and enhancer of zeste (CLF) establish “bivalent chromatin marks” at the silent AGAMOUS locus. *Nucleic Acids Research*. https://doi.org/10.1093/nar/gkm464

Sanchez, D. H., & Paszkowski, J. (2014). Heat-Induced Release of Epigenetic Silencing Reveals the Concealed Role of an Imprinted Plant Gene. *PLoS Genetics*. https://doi.org/10.1371/journal.pgen.1004806

Schelbert, S., Aubry, S., Burla, B., Agne, B., Kessler, F., Krupinska, K., & Hortensteiner, S. (2009). Pheophytin Pheophorbide Hydrolase (Pheophytinase) Is Involved in Chlorophyll Breakdown during Leaf Senescence in Arabidopsis. *THE PLANT CELL ONLINE*. https://doi.org/10.1105/tpc.108.064089

Schindelin, J., Arganda-Carreras, I., Frise, E., Kaynig, V., Longair, M., Pietzsch, T., … Cardona, A. (2012). Fiji: An open-source platform for biological-image analysis. *Nature Methods*. https://doi.org/10.1038/nmeth.2019

Scholthof, K.-B. G., Irigoyen, S., Catalan, P., & Mandadi, K. (2018). Brachypodium: A monocot grass model system for plant biology. *The Plant Cell*. https://doi.org/10.1105/tpc.18.00083

Schotta, G., Ebert, A., Dorn, R., & Reuter, G. (2003). Position-effect variegation and the genetic dissection of chromatin regulation in Drosophila. *Seminars in Cell and Developmental Biology*. https://doi.org/10.1016/S1084-9521(02)00138-6

Schubert, H. L., Blumenthal, R. M., & Cheng, X. (2003). Many paths to methyltransfer: A chronicle of convergence. *Trends in Biochemical Sciences*. https://doi.org/10.1016/S0968-0004(03)00090-2

Sherman, J. D., & Talbert, L. E. (2002). Vernalization-induced changes of the DNA methylation pattern in winter wheat. *Genome*. https://doi.org/10.1139/g01-147

Shibuya, K., Fukushima, S., & Takatsuji, H. (2009). RNA-directed DNA methylation induces transcriptional activation in plants. *Proceedings of the National Academy of Sciences*. https://doi.org/10.1073/pnas.0809294106

Silveira, A. B., Trontin, C., Cortijo, S., Barau, J., Del Bem, L. E. V., Loudet, O., … Vincentz, M. (2013). Extensive Natural Epigenetic Variation at a De Novo Originated Gene. *PLoS Genetics*. https://doi.org/10.1371/journal.pgen.1003437

Slotkin, R. K., Vaughn, M., Borges, F., Tanurdžić, M., Becker, J. D., Feijó, J. A., & Martienssen, R. A. (2009). Epigenetic Reprogramming and Small RNA Silencing of Transposable Elements in Pollen. *Cell*. https://doi.org/10.1016/j.cell.2008.12.038

Song, Y., Ji, D., Li, S., Wang, P., Li, Q., & Xiang, F. (2012). The dynamic changes of DNA methylation and histone modifications of salt responsive transcription factor genes in soybean. *PLoS ONE*. https://doi.org/10.1371/journal.pone.0041274

Soppe, W. J. J., Jacobsen, S. E., Alonso-Blanco, C., Jackson, J. P., Kakutani, T., Koornneef, M., & Peeters, A. J. M. (2000). The late flowering phenotype of fwa mutants is caused by gain-of-function epigenetic alleles of a homeodomain gene. *Molecular Cell*. https://doi.org/10.1016/S1097-2765(05)00090-0

Steward, N., Ito, M., Yamaguchi, Y., Koizumi, N., & Sano, H. (2002). Periodic DNA methylation in maize nucleosomes and demethylation by environmental stress. *Journal of Biological Chemistry*. https://doi.org/10.1074/jbc.M204050200

Stroud, H., Do, T., Du, J., Zhong, X., Feng, S., Johnson, L., … Jacobsen, S. E. (2014). Non-CG methylation patterns shape the epigenetic landscape in Arabidopsis. *Nature Structural and Molecular Biology*. https://doi.org/10.1038/nsmb.2735

Tan, F., Zhou, C., Zhou, Q., Zhou, S., Yang, W., Zhao, Y., … Zhou, D.-X. (2016). Analysis of Chromatin Regulators Reveals Specific Features of Rice DNA Methylation Pathways. *Plant Physiology*. https://doi.org/10.1104/pp.16.00393

Tang, K., Lang, Z., Zhang, H., & Zhu, J. K. (2016). The DNA demethylase ROS1 targets genomic regions with distinct chromatin modifications. *Nature Plants*. https://doi.org/10.1038/nplants.2016.169

Tang, X., Wang, Q., & Huang, X. (2018). Chilling-induced DNA Demethylation is associated with the cold tolerance of Hevea brasiliensis. *BMC Plant Biology*. https://doi.org/10.1186/s12870-018-1276-7

Tao, J., Liang, W., An, G., & Zhang, D. (2018). *OsMADS6* Controls Flower Development by Activating Rice *FACTOR OF DNA METHYLATION LIKE1*. *Plant Physiology*. https://doi.org/10.1104/pp.18.00017

Tuan, P. A., Kumar, R., Rehal, P. K., Toora, P. K., & Ayele, B. T. (2018). Molecular mechanisms underlying abscisic acid/gibberellin balance in the control of seed dormancy and germination in cereals. *Frontiers in Plant Science*. https://doi.org/10.3389/fpls.2018.00668

Veiseth, S. V., Rahman, M. A., Yap, K. L., Fischer, A., Egge-Jacobsen, W., Reuter, G., … Thorstensen, T. (2011). The SUVR4 histone lysine methyltransferase binds ubiquitin and converts H3K9me1 to H3K9me3 on transposon chromatin in arabidopsis. *PLoS Genetics*. https://doi.org/10.1371/journal.pgen.1001325

Verelst, W., Bertolini, E., De Bodt, S., Vandepoele, K., Demeulenaere, M., Pè, M. E., & Inzé, D. (2013). Molecular and physiological analysis of growth-limiting drought stress in brachypodium distachyon leaves. *Molecular Plant*. https://doi.org/10.1093/mp/sss098

Viggiano, L., & de Pinto, M. (2017). Dynamic DNA Methylation Patterns in Stress Response (pp. 281–302). https://doi.org/10.1007/978-3-319-55520-1_15

Vogel, J., & Hill, T. (2008). High-efficiency Agrobacterium-mediated transformation of Brachypodium distachyon inbred line Bd21-3. *Plant Cell Reports*. https://doi.org/10.1007/s00299-007-0472-y

Vogel, J. P., Garvin, D. F., Mockler, T. C., Schmutz, J., Rokhsar, D., Bevan, M. W., … Baxter, I. (2010). Genome sequencing and analysis of the model grass Brachypodium distachyon. *Nature*. https://doi.org/10.1038/nature08747

Wada, Y., Miyamoto, K., Kusano, T., & Sano, H. (2004). Association between up-regulation of stress-responsive genes and hypomethylation of genomic DNA in tobacco plants. *Molecular Genetics and Genomics*. https://doi.org/10.1007/s00438-004-1018-4

Wada, Y., Ohya, H., Yamaguchi, Y., Koizumi, N., & Sano, H. (2003). Preferential de Novo Methylation of Cytosine Residues in Non-CpG Sequences by a Domains Rearranged DNA Methyltransferase from Tobacco Plants. *Journal of Biological Chemistry*. https://doi.org/10.1074/jbc.M303892200

Wang, H., Wang, H., Shao, H., & Tang, X. (2016). Recent Advances in Utilizing Transcription Factors to Improve Plant Abiotic Stress Tolerance by Transgenic Technology. *Frontiers in Plant Science*. https://doi.org/10.3389/fpls.2016.00067

Wang, W., Qin, Q., Sun, F., Wang, Y., Xu, D., Li, Z., & Fu, B. (2016). Genome-Wide Differences in DNA Methylation Changes in Two Contrasting Rice Genotypes in Response to Drought Conditions. *Frontiers in Plant Science*. https://doi.org/10.3389/fpls.2016.01675

Wang, W. S., Pan, Y. J., Zhao, X. Q., Dwivedi, D., Zhu, L. H., Ali, J., … Li, Z. K. (2011). Drought-induced site-specific DNA methylation and its association with drought tolerance in rice (Oryza sativa L.). *Journal of Experimental Botany*. https://doi.org/10.1093/jxb/erq391

Wei, L., Gu, L., Song, X., Cui, X., Lu, Z., Zhou, M., … Cao, X. (2014). Dicer-like 3 produces transposable element-associated 24-nt siRNAs that control agricultural traits in rice. *Proceedings of the National Academy of Sciences*. https://doi.org/10.1073/pnas.1318131111

Wen, F., Wu, X., Li, T., Jia, M., Liu, X., Li, P., … Yue, X. (2017). Genome-wide survey of heat shock factors and heat shock protein 70s and their regulatory network under abiotic stresses in Brachypodium distachyon. *PLoS ONE*. https://doi.org/10.1371/journal.pone.0180352

Wicker, T., Gundlach, H., Spannagl, M., Uauy, C., Borrill, P., Ramírez-González, R. H., … Choulet, F. (2018). Impact of transposable elements on genome structure and evolution in bread wheat. *Genome Biology*. https://doi.org/10.1186/s13059-018-1479-0

Widom, J. (1992). A relationship between the helical twist of DNA and the ordered positioning of nucleosomes in all eukaryotic cells. *Proceedings of the National Academy of Sciences*. https://doi.org/10.1073/pnas.89.3.1095

Woo, H. R., Dittmer, T. A., & Richards, E. J. (2008). Three SRA-domain methylcytosine-binding proteins cooperate to maintain global CpG methylation and epigenetic silencing in

arabidopsis. *PLoS Genetics*. https://doi.org/10.1371/journal.pgen.1000156
Woodcock, C. L., Skoultchi, A. I., & Fan, Y. (2006). Role of linker histone in chromatin structure and function: H1 stoichiometry and nucleosome repeat length. *Chromosome Research*. https://doi.org/10.1007/s10577-005-1024-3
Woods, D. P., Ream, T. S., Bouché, F., Lee, J., Thrower, N., Wilkerson, C., & Amasino, R. M. (2017). Establishment of a vernalization requirement in Brachypodium distachyon requires REPRESSOR OF VERNALIZATION1. *Proceedings of the National Academy of Sciences of the United States of America*. https://doi.org/10.1073/pnas.1700536114
Xu, D., Bai, J., Duan, Q., Costa, M., & Dai, W. (2009). Covalent modifications of histones during mitosis and meiosis. *Cell Cycle*. https://doi.org/10.4161/cc.8.22.9908
Yamaguchi-Shinozaki, K. (1994). A Novel cis-Acting Element in an Arabidopsis Gene Is Involved in Responsiveness to Drought, Low-Temperature, or High-Salt Stress. *THE PLANT CELL ONLINE*. https://doi.org/10.1105/tpc.6.2.251
Yamamuro, C., Miki, D., Zheng, Z., Ma, J., Wang, J., Yang, Z., … Zhu, J. K. (2014). Overproduction of stomatal lineage cells in Arabidopsis mutants defective in active DNA demethylation. *Nature Communications*. https://doi.org/10.1038/ncomms5062
Ye, R., Wang, W., Iki, T., Liu, C., Wu, Y., Ishikawa, M., … Qi, Y. (2012). Cytoplasmic Assembly and Selective Nuclear Import of Arabidopsis ARGONAUTE4/siRNA Complexes. *Molecular Cell*. https://doi.org/10.1016/j.molcel.2012.04.013
Zadoks, J. C., Chang, T. T., & Konzak, C. F. (1974). A decimal code for the growth stages of cereals. *Weed Research*. https://doi.org/10.1111/j.1365-3180.1974.tb01084.x
Zemach, A., Kim, M. Y., Hsieh, P. H., Coleman-Derr, D., Eshed-Williams, L., Thao, K., … Zilberman, D. (2013). The arabidopsis nucleosome remodeler DDM1 allows DNA methyltransferases to access H1-containing heterochromatin. *Cell*. https://doi.org/10.1016/j.cell.2013.02.033
Zhang, H., Lang, Z., & Zhu, J. K. (2018). Dynamics and function of DNA methylation in plants. *Nature Reviews Molecular Cell Biology*. https://doi.org/10.1038/s41580-018-0016-z
Zhang, H., & Zhu, J. K. (2012). Active DNA demethylation in plants and animals. *Cold Spring Harbor Symposia on Quantitative Biology*. https://doi.org/10.1101/sqb.2012.77.014936
Zhang, X., Yazaki, J., Sundaresan, A., Cokus, S., Chan, S. W. L., Chen, H., … Ecker, J. R. R. (2006). Genome-wide High-Resolution Mapping and Functional Analysis of DNA Methylation in Arabidopsis. *Cell*. https://doi.org/10.1016/j.cell.2006.08.003
Zhong, S., Fei, Z., Chen, Y. R., Zheng, Y., Huang, M., Vrebalov, J., … Giovannoni, J. J. (2013). Single-base resolution methylomes of tomato fruit development reveal epigenome modifications associated with ripening. *Nature Biotechnology*. https://doi.org/10.1038/nbt.2462
Zhong, X., Du, J., Hale, C. J., Gallego-Bartolome, J., Feng, S., Vashisht, A. A., … Jacobsen, S. E. (2014). Molecular mechanism of action of plant DRM de novo DNA methyltransferases. *Cell*. https://doi.org/10.1016/j.cell.2014.03.056
Zhou, C., Wang, C., Liu, H., Zhou, Q., Liu, Q., Guo, Y., … Zhou, D. X. (2018). Identification and analysis of adenine N6-methylation sites in the rice genome. *Nature Plants*. https://doi.org/10.1038/s41477-018-0214-x
Zhou, M., & Law, J. A. (2015). RNA Pol IV and V in gene silencing: Rebel polymerases evolving away from Pol II's rules. *Current Opinion in Plant Biology*. https://doi.org/10.1016/j.pbi.2015.07.005
Zhou, S., Liu, X., Zhou, C., Zhou, Q., zhao, Y., Li, G., & Zhou, D.-X. (2016). Cooperation

between the H3K27me3 chromatin marker and non-CG methylation in epigenetic regulation. *Plant Physiology*. https://doi.org/10.1104/pp.16.01238

Zhou, Y., He, R., Guo, Y., Liu, K., Huang, G., Peng, C., … Duan, L. (2019). A novel ABA functional analogue B2 enhances drought tolerance in wheat. *Scientific Reports*. https://doi.org/10.1038/s41598-019-39013-8

Supplementary Table 3.1 *B. distachyon* epigenome regulatory gene homologs

A. thaliana gene name	Function in *A. thaliana*	*A. thaliana* gene reference	*B. distachyon* gene reference	Proposed *B. distachyon* gene name	% identity
CMT1	Probable DNA methyltransferase	AT1G80740.1	BRADI_1g68985v3; XM_010231902.3	BdCMT1	45.33
CMT2	DNA methyltransferase	AT4G19020.1	BRADI_1g66167v3; XM_014897119.2	BdCMT2	50.50
CMT3	DNA methyltransferase	AT1G69770.1	BRADI_3g21450v3; XM_010236308.3	BdCMT3	47.10
DRM2	DNA methyltransferase	AT5G14620.1	BRADI_4g05680v3; XM_010238895.3	BdDRM2	51.47
DRM3	Catalytically inactive DNA methyltransferase	AT3G17310.2	BRADI_2g38577v3; XM_003569029.3	BdDRM3	41.52
MET1	DNA methyltransferase	AT5G49160.1	BRADI_1g05380v3; XM_003559258.4	BdMET1A	51.70
			BRADI_1g55287v3; XM_024456904.1	BdMET1B	54.76
ROS1	DNA glycosylase/lyase	AT2G36490.1	BRADI_2g23797v3; XM_014899063.2	BdROS1A	56.99
			BRADI_4g16620v3; XM_014903096.2	BdROS1B	56.44
SUVR4	Histone-lysine N-methyltransferase	AT3G04380.1	BRADI_3g48970v3; XM_003572674.4	BdSUVR4	51.18

Supplementary Table 3.2 Annotated repetitive elements in select UBI:BdDRM2 Line 3 DEGs.

Gene ID	Gene Position	RefSeq Description	Repeat	Repeat length	Repeat Position	Repeat feature location
BRADI_2g02400v3	Bd2: 1,630,992-1,631,692 (-)	16.9 kDa class I heat shock protein 3	(GGCGTC)n	39	Bd2:1631489-1631527 (+)	exon
BRADI_2g02410v3	Bd2: 1,631,990-1,632,765 (+)	16.9 kDa class I heat shock protein 3	*NA*	*NA*	*NA*	*NA*
BRADI_2g05374v3	Bd2: 3,913,040-3,913,537 (-)	17.5 kDa class II heat shock protein	(CGC)n	31	Bd2:3913423-3913453 (+)	exon
BRADI_3g58590v3	Bd3: 57,826,566-57,827,820 (-)	24.1 kDa heat shock protein	(GA)n	17	Bd3:57826752-57826768 (+)	3' UTR
			(CCG)n	39	Bd3:57827151-57827189 (+)	exon
BRADI_1g53850v3	Bd1: 52,437,476-52,438,467 (+)	17.9 kDa class I heat shock protein	GA-rich	31	Bd1:52437886-52437916 (+)	exon
			(CCTG)n	26	Bd1:52438154-52438179 (+)	intron
BRADI_2g23797v3	Bd2: 21,543,282-21,553,515 (+)	Brachypodium distachyon protein ROS1	*NA*	*NA*	*NA*	*NA*
BRADI_4g16620v3	Bd4: 17,468,587-17,484,078 (+)	ENDO3c domain-containing protein	trep216	128	Bd4:17468193-17468320 (-)	promoter
			(TTTTCT)n	56	Bd4:17468846-17468901 (+)	intron
			(CAT)n	29	Bd4:17469823-17469851 (+)	exon
			trep2027	120	Bd4:17472220-17472339 (+)	intron
			(GCAT)n	35	Bd4:17475761-17475795 (+)	intron
			Zm_AC148173.2_1L	681	Bd4:17481580-17482260 (+)	intron
			SC-5	132	Bd4:17482339-17482470 (-)	intron
			A-rich	35	Bd4:17483607-17483641 (+)	3' UTR

Supplementary Table 3.3 Primers used in this study.

Gene target	Primer name	Sequence (5'-3')	Amplicon size (bp)	Source
BdDRM2	qp_DRM2_F	TGGGTTGGCAAGAACAAGGT	97	Present study
	qp_DRM2_R	CTGTCTTGCCGATTCCCCTT		
BdSamDC	qp_SamDC_F	TGCTAATCTGCTCCAATGGC	190	Hong et al., 2008
	qp_SamDC_R	GACGCAGCTGACCACCTAGA		
BdUBC18	qp_UBC18_F	GGAGGCACCTCAGGTCATTT	193	Hong et al., 2008
	qp_UBC18_R	ATAGCGGTCATTGTCTTGCG		

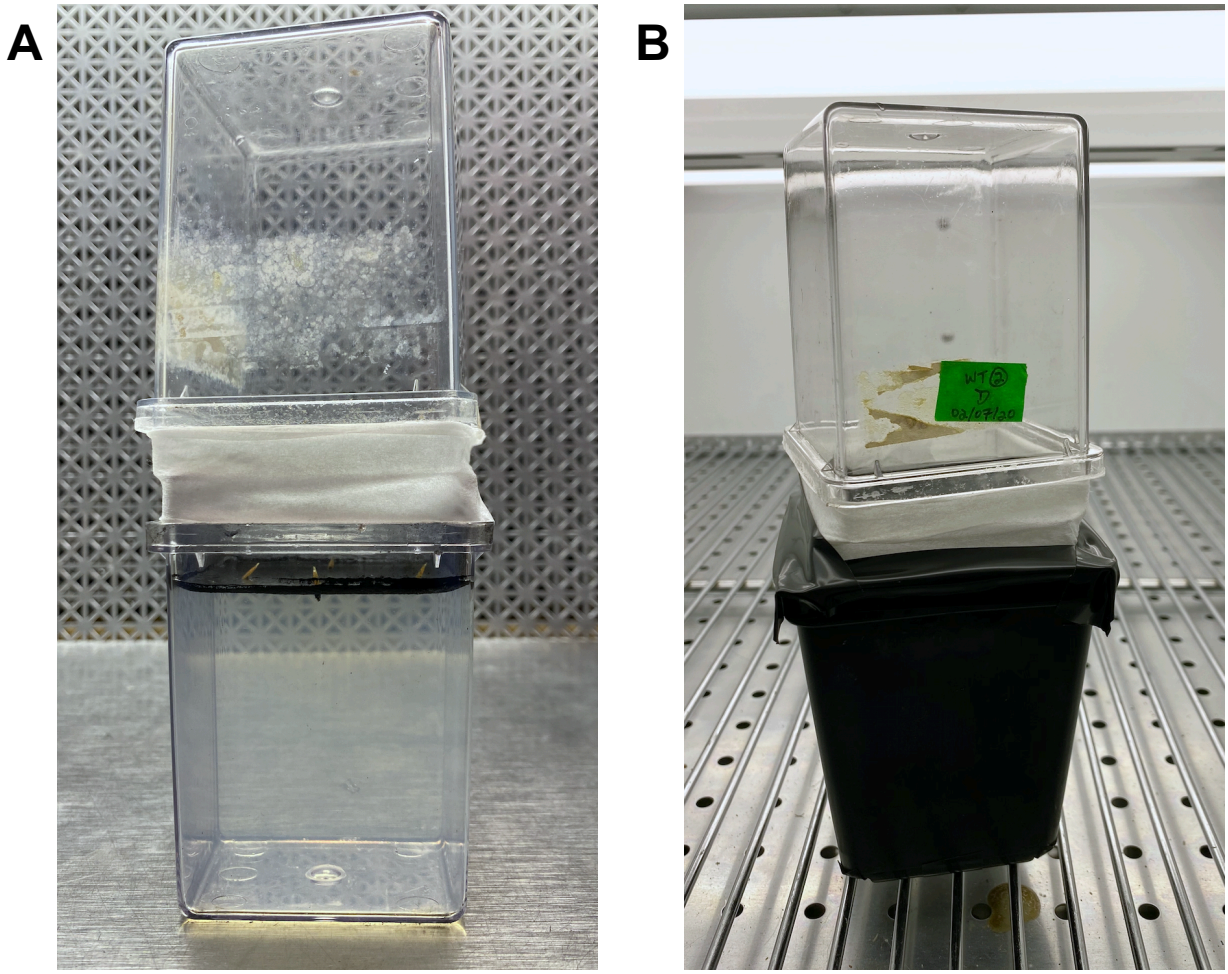

Supplementary Figure 3.1. Root growth chambers (RGCs) used to analyze developing *B. distachyon* root growth. (A) Sealed RGC with four sterilized *B. distachyon* seeds planted, one on each face. After planting, RGCs were moved to an environmental growth chamber (22°C, 16h photoperiod) with the basal plant culture box covered to minimize root exposure to light **(B)**.